MOLECULAR AND CELLULAR BIOLOGY, May 2010, p. 2264–2279 Vol. 30, No. 9
0270-7306/10/$12.00 doi:10.1128/MCB.01450-08

The RasGAP Proteins Ira2 and Neurofibromin Are Negatively Regulated by Gpb1 in Yeast and ETEA in Humans▽

Vernon T. Phan,[1]† Vivianne W. Ding,[1] Fenglei Li,[2] Robert J. Chalkley,[2] Alma Burlingame,[2] and Frank McCormick[1]*

UCSF Helen Diller Family Comprehensive Cancer Center, 2340 Sutter Street, San Francisco, California 94115,[1] *and Department of Pharmaceutical Chemistry and Mass Spectrometry Facility, University of California, San Francisco, San Francisco, California 94143*[2]

Received 15 September 2008/Returned for modification 12 November 2008/Accepted 9 February 2010

The neurofibromatosis type 1 (NF1) gene encodes the GTPase-activating protein (GAP) neurofibromin, which negatively regulates Ras activity. The yeast *Saccharomyces cerevisiae* has two neurofibromin homologs, Ira1 and Ira2. To understand how these proteins are regulated, we utilized an unbiased proteomics approach to identify Ira2 and neurofibromin binding partners. We demonstrate that the Gpb1/Krh2 protein binds and negatively regulates Ira2 by promoting its ubiquitin-dependent proteolysis. We extended our findings to show that in mammalian cells, the ETEA/UBXD8 protein directly interacts with and negatively regulates neurofibromin. ETEA contains both UBA and UBX domains. Overexpression of ETEA downregulates neurofibromin in human cells. Purified ETEA, but not a mutant of ETEA that lacks the UBX domain, ubiquitinates the neurofibromin GAP-related domain *in vitro*. Silencing of *ETEA* expression increases neurofibromin levels and downregulates Ras activity. These findings provide evidence for conserved ubiquitination pathways regulating the RasGAP proteins Ira2 (in yeast) and neurofibromin (in humans).

Neurofibromatosis type 1 (NF1) is an autosomal dominant genetic disease that affects 1 in 3,500 individuals worldwide. Individuals with NF1 are predisposed to develop multiple benign and malignant neurofibromas as well as gliomas, pheochromocytomas, and myeloid leukemias (2, 32). Neurofibromin, the *NF1* gene product, negatively regulates Ras activity by facilitating the hydrolysis of active RasGTP to inactive RasGDP through its GTPase-activating protein (GAP) domain (3, 25). Loss of neurofibromin results in hyperactive Ras signaling and activation of downstream effectors, including the Raf–MEK–extracellular signal-regulated kinase (ERK) and phosphatidylinositol 3-kinase (PI3K)–AKT pathways (35, 45).

Regulation of neurofibromin itself is still poorly understood. Phosphorylation by protein kinase C (PKC) increases in the RasGAP activity in response to epidermal growth factor (EGF) signaling (24). Furthermore, neurofibromin can be phosphorylated on serine residues when IgM is cross-linked, although the kinase that is responsible for the regulation is unknown (5). Neurofibromin can be degraded by the proteasome when cells are stimulated with growth factors that activate both G-protein-coupled receptors and receptor tyrosine kinases (7). Although neurofibromin is ubiquitinated and degraded, the ubiquitin-related enzyme responsible remains to be identified. Taken together, these findings suggest that neurofibromin is controlled by both protein kinases and ubiquitin-related enzymes and that identifying new protein candidates that regulate neurofibromin is crucial to advancing the understanding of NF1.

In the yeast *Saccharomyces cerevisiae*, there are two *NF1*-like genes, *IRA1* and *IRA2*, which encode Ira1 and Ira2 proteins, respectively. Ira proteins are negative regulators of Ras1 and Ras2 and were first identified as components of the adenylyl cyclase-cyclic AMP (cAMP)-protein kinase A (PKA) pathway (40). Deletion of Ras1 and Ras2 in yeast cells causes a G_0 arrest due to lack of adenylyl cyclase activity. However, hyperactivation of Ras, either by *IRA* gene deletion or by expression of activated *RAS* alleles, activates the adenylyl cyclase-cAMP-PKA pathway. Constitutive Ras activation causes yeast cells to die at high temperature. The Ras-induced heat shock sensitivity is reversed when the GAP domain of human neurofibromin is expressed in the *ira*-deleted yeast strains (3, 43). In yeast, addition of glucose can trigger activation of adenylyl cyclase activity via the Gpr1/Gpa2 pathway (10, 11). Recently, reported studies showed that glucose stimulation increases Ras-GTP levels in yeast (11, 34). Similarly, deletion of *GPR1* or *GPA2* causes Ras activation, suggesting that the Gpr1/Gpa2 pathway might regulate Ras activity (11). Gpr1 binds to the Gα subunit Gpa2 and its Gβ-like subunits Gpb1/Krh2 and Gpb2/Krh1 to control adenylyl cyclase activity (16). Gpb1/Krh2 and Gpb2/Krh1 both possess C-terminal Kelch repeat domains but have unique N-terminal domains (13, 16). The Kelch repeat domain is predicted to have a protein folding similar to that of the WD40 repeat domain that is commonly found in GPCR Gβ subunits, TAFII transcription factors, and E3 ubiquitin ligases (19, 30). A role for Gpb1/Krh2 and Gpb2/Krh1 in the positive regulation of Ira proteins has been proposed, but the molecular mechanism responsible for this regulation remains unknown (15).

To better understand Ira/neurofibromin function, we initiated an unbiased proteomic purification approach to identify

* Corresponding author. Mailing address: UCSF Helen Diller Family, Comprehensive Cancer Center, 2340 Sutter Street, San Francisco, CA 94115. Phone: (415) 502-1710. Fax: (415) 502-1712. E-mail: address: mccormick@cc.ucsf.edu.

† Present address: Genentech, Inc., 1 DNA Way, South San Francisco, CA 94080.

▽ Published ahead of print on 12 February 2010.

TABLE 1. Yeast strains used in this study[a]

Strain	Genotype	Source or reference
W303 background		
VPD1	*ade2 his3 leu2 trp1 ura3 can1 ira1*::*LEU2*	This study
VPD2	*ade2 his3 leu2 trp1 ura3 can1 ira2*::*KanMx*	This study
VPD1.2	*ade2 his3 leu2 trp1 ura3 can1 ira1*::*LEU2 ira2*::*KanMx*	This study
S288c background		
IRA2HA		Open Biosystems
G1TAP	*his3 leu2 met15 ura3 GPB1-TAP*::*HIS3*	14
IRA2TAP	*his3 leu2 met15 ura3 IRA2-TAP*::*HIS3*	14
VP2.3F	*ade2 his3 leu2 trp1 ura3 can1 IRA2-3FLAG*::*KanMx*	This study
VP2.3FDG1.7	*ade2 his3 leu2 trp1 ura3 can1 IRA2-3FLAG*::*KanMx gpb1-TAP*::*LEU2*	This study
VP2.3FDG1.10	*ade2 his3 leu2 trp1 ura3 can1 IRA2-3FLAG*::*KanMx gpb1-TAP*::*LEU2*	This study
VPG1TP2F	*his3 leu2 met15 ura3 GPB1-TAP*::*HIS3 IRA2-3FLAG*::*KanMx*	This study
VPG1TPD2	*his3 leu2 met15 ura3 GPB1-TAP*::*HIS3 ira2*::*KanMx*	This study
VP2TPG1F	*his3 leu2 met15 ura3 IRA2-TAP*:*HIS3 GPB1-3FLAG*::*KanMx*	This study
VP2TPD2	*his3 leu2 met15 ura3 IRA2-TAP*:*HIS3 ira2*::*KanMx*	This study
VPCT13F	*his3 leu2 met15 ura3 CCT1-3FLAG*::*KanMx*	This study
VPG1V5	*his3 leu2 met15 ura3 GPB1-V5*::*HIS3*	This study

[a] Yeast strains were derived from W303a, except the IRA2-HA-tagged strain and the TAP-tagged strains, which were purchased from the TAP tag library (Open Biosystems) (14).

novel Ira/neurofibromin binding proteins. We identified that proteins containing ubiquitin-associated domains can negatively regulate Ira2 and neurofibromin. In yeast, we found that Gpb1/Krh2 negatively regulates and promotes Ira2 degradation (we will refer to Gpb1/Krh2 as Gpb1). Similarly, we identified ETEA as a human ubiquitin-associated protein that negatively regulates neurofibromin levels. RNA interference (RNAi) targeting of *ETEA* expression caused an upregulation of neurofibromin, reduced Ras activities, and downregulated both the ERK and the AKT pathways. Therefore, these data reveal critical conserved ubiquitination pathways that regulate the RasGAP proteins Ira2 (in yeast) and neurofibromin (in humans).

MATERIALS AND METHODS

Strains and plasmids. All of the yeast strains described in this article are listed in Table 1. The double-epitope-tagged strains described in this article were generated from the TAP-tagged parental strains, and the second gene was epitope tagged using PCR-based FLAG tagging techniques previously described (22). All plasmid constructs used in this article were generated by standard PCR targeting techniques and cloned into Gateway entry and destination vectors (Invitrogen).

Tandem affinity purification and mass spectrometry. Yeast cells endogenously expressing either IRA2-TAP or GPB1-TAP or 293T cells expressing TAP-NF1 fragments were used for the tandem affinity purification (TAP) experiments. The purification scheme was adapted from references 14 and 33. Briefly, either yeast cell extracts from 6 to 10 litters of cells grown to log phase and expressing Ira2-TAP or Gpb1-TAP or lysates from 293T stably expressed NF1-TAP fragments were incubated at 4°C with 500 μl of packed IgG-conjugated glutathione resin (Amersham). Resin beads were washed, and protein complexes were then eluted from the IgG resin in calmodulin binding buffer supplemented with 50 units of tobacco etch virus (TEV) protease (Invitrogen). The second round of affinity purification was performed using 400 μl of calmodulin resin (Amersham). The protein complexes were then eluted with 2 200-μl volumes of elution buffer, precipitated, and separated by precast PAGE. Separated protein bands were excised and digested with trypsin and analyzed for matched protein sequences against the protein database. The experimental methods for protein band sequencing analysis were described previously (33).

Immunoprecipitation and immunoblotting. Total cell lysates were prepared in cell lysis buffer containing 20 mM Tris-HCl, pH 7.5, 500 mM NaCl, 0.1% NP-40, 50 mM NaF, 1 mM dithiothreitol (DTT), 1 mM Na_3VO_4, and a protease inhibitor cocktail (this buffer is hereinafter referred to as "lysis buffer"). After normalization of protein concentrations, approximately 300 to 500 μg of total protein samples was immunoprecipitated with the indicated antibodies. Sample mixtures were rotated at 4°C for 2 h. After three washes with the lysis buffer, the proteins bound to beads were released by boiling in 40 μl of 1× SDS-PAGE sample buffer for 10 min. All the immunoprecipitation experiments performed were done with normalized protein concentrations. The samples were then resolved by precast PAGE, followed by immunoblotting using the indicated antibodies. Densitometry of the resulting bands was done by using Bio-Rad Quantity One software (Hercules, CA), and protein amounts were corrected based on actin values. The final values presented are averages of results from three independent densitometry experiments.

***In vitro* translation.** The TNT quick coupled transcription/translation system (Promega) was used to detect *in vitro* protein-protein interactions. All experiments described were performed according to the manufacturer's instructions. *In vitro* reactions involving [^{35}S]methionine labeling were terminated by adding 500 μl lysis buffer. Antibodies and conjugated beads were added to the radioactive protein mixture, and immunoprecipitation was performed. The beads were washed four times with 1 ml of lysis buffer. The proteins bound to beads were released by boiling in 50 μl of 1× SDS-PAGE sample buffer for 10 min. The samples were then resolved by precast PAGE, followed by visualization with a Storm 860 PhosphorImager (Molecular Dynamics).

***In vitro* ubiquitination of Ira2 and the neurofibromin GRD.** Gpb1-TAP complexes were purified as described previously except that the final calmodulin binding step was omitted from the Gpb1 complex preparation. The reactions were carried out at 30°C for 1.5 h in 50 μl reaction buffer (40 mM Tris-HCl, pH 7.5, 2 mM DTT, 5 mM $MgCl_2$) containing 2 or 4 μg of ubiquitin (U-100; Boston Biochem) or 4 μg of mutant ubiquitin (ubiØ), 5 mM ATP, a complex consisting of 1.5 μg/ml activated E1 and 20 μg/ml UbcH5, and a complex consisting of purified Flag-Ira2 and 200 μg of TAP-cleaved purified Gpb1 protein as E3 sources. The reactions were terminated by adding 500 μl lysis buffer. After addition of 20 μl of M2 Flag agarose-conjugated beads, the samples were rotated at 4°C for 2 h. The beads were washed four times with 1 ml of pulldown buffer, followed by three washes with 1× phosphate-buffered saline (PBS). The proteins bound to Flag beads were released by boiling in 50 μl of 1× SDS-PAGE sample buffer. The samples were then resolved by precast PAGE, followed by immunoblotting using anti-His or anti-Flag antibodies.

For the ubiquitin assay of the neurofibromin GAP-related domain (GRD), an *in vitro*-[^{35}S]methionine-labeled neurofibromin GRD was immunoprecipitated with glutathione-conjugated Sepharose beads and used as substrates. The reactions were carried out at 30°C for 1.5 h in 50 μl reaction buffer (same as above) containing 10 μg of ubiquitin (U-100; Boston Biochem), 5 mM ATP, a complex consisting of 1.5 μg/ml activated E1 and 20 μg/ml UbcH5, and a complex consisting of 100 μg of purified green fluorescent protein (GFP)-glutathione *S*-transferase (GST), ETEA-GFP, or ETEA ΔUBX protein. The reactions were terminated by adding 500 μl lysis buffer. Samples were immunoprecipitated at 4°C for 2 h. The beads were washed four times with 1 ml of lysis buffer and then three times with 1× PBS. The [^{35}S]methionine-labeled neurofibromin GRD

complexes were released by boiling in 50 μl of 1× SDS-PAGE sample buffer for 10 min. The samples were then resolved by NuPAGE, followed by visualization with a Storm 860 PhosphorImager.

Cycloheximide chase experiments. To examine the effect of Gpb1 on Ira2 stability, exponentially growing wild-type (WT) or *gpb1*Δ yeast strains were treated with cycloheximide at a final concentration of 50 mg/ml to inhibit *de novo* protein synthesis. Cells were collected and washed at the time points indicated. Total cell extracts were prepared, and the protein concentrations were determined. Samples were analyzed by immunoblotting for Ira2 and Gpb1 with anti-Flag or anti-TAP antibodies. To examine the effect of ETEA or ETEA UBXΔ on neurofibromin stability, 293T cells were treated with cycloheximide at a final concentration of 150 μg/ml. Samples were terminated at the 0-, 4-, 8-, 12-, and 15-h time points as indicated. The protein concentrations were normalized, and 10 μg of total protein from each sample was immunoblotted with antineurofibromin, anti-GFP, anti-V5, and antiactin antibodies. Densitometry of the resulting bands was done by using Bio-Rad Quantity One software (Hercules, CA), and protein amounts were corrected based on actin values. The final values presented are averages of results from three independent densitometry experiments.

shRNA stable cell lines. 293T or BT459 cells were seeded in 6-well dishes 24 h prior to transient transfection with 4 μg of total short hairpin RNA (shRNA) DNA plasmids using 10 μl of Lipofectamine reagent (Invitrogen). The three human pSM2 retroviral shRNAmir plasmids targeting *ETEA* (clones V2HS_80576, V2HS_80578, and V2HS_80580) were purchased from Open Biosystems. In order to generate stable cell lines expressing the shRNA plasmids, 48 to 72 h after transfections, cells were replated in Dulbecco's modified Eagle's medium (DMEM) (supplemented with 10% fetal bovine serum [FBS]) plus 1 μg/ml puromycin for more than 10 days. Densitometry of the resulting bands was done by using Bio-Rad Quantity One software (Hercules, CA), and protein amounts were corrected based on actin values. The final values presented were averages of results from three independent densitometry experiments.

RasGTP detection. Total cellular extracts were prepared and used for immunoprecipitation with the GST-fused Ras binding domain-conjugated glutathione resin. The experimental procedures were previously described (33). For yeast RasGTP pulldown experiments, membranes were immunoblotted with anti-Ras2 antibody. For RasGTP pulldown experiments in 293T cells, the panRAS antibody was used to determine RasGTP levels.

RNA extraction and quantification. Total RNA was isolated using a RiboPure yeast kit from Ambion (catalog no. AM1024). Quantitative reverse transcription-PCRs (qRT-PCRs) were run in triplicate using the ABI Prism 7500 sequence detector system by using SYBR green qPCR master mix (Applied Biosystems, Foster City, CA). The level of each transcript was quantified by the $\Delta\Delta C_T$ method, and expression of *ACT1* was used as an internal control for all of the samples. The levels of *HSP12*, *CTT1*, and *GPB1* expression are indicated as *n*-fold increases relative to the levels for *HSP12*, *CTT1*, and *GPB1* expression in WT cells and cells receiving control plasmids grown under the same conditions. The average values for WT cells and cells receiving control plasmids were normalized to 1. The experiments were performed and repeated with two sets of primers per gene to exclude nonspecific activity.

Reagents and antibodies. MG132 was from Calbiochem. Anti-Flag M2 (unconjugated) and anti-Flag M2 conjugated beads were from Sigma. Anti-Ydj1 (sc-23749), anti-NF1 (sc-67), anti-GFP (sc-8334), antihemagglutinin (anti-HA) (sc-805), anti-p120GAP, and anti-RAS2 were from Santa Cruz Biotechnology. Antiubiquitin antibodies were from Zymed and Abcam. Anti-V5 was from Abcam. Anti-Ras (panRas) was from BD Biosciences. Antiactin was from Sigma. Recombinant ubiquitin proteins were from Boston Biochem.

RESULTS

Analysis of Ira2-TAP fusion protein and purification of Ira2 binding partners. To identify protein complexes that bind to Ira2, we utilized a yeast strain with endogenous Ira2 fused at the C terminus with the TAP tag. We characterized the *IRA2-TAP* yeast strain to determine whether the TAP-tagged fusion protein interfered with Ira2 activity. Western blotting showed that the *IRA2-TAP* yeast strain endogenously expressed the Ira2-TAP fusion protein (Fig. 1A). Loss of Ira2 activates Ras and results in heat sensitivity (37, 38). Therefore, we examined whether loss of the Ira2-TAP protein would result in heat shock sensitivity. We generated an *ira2* mutant strain (*ira2-TAP*Δ) and compared its heat sensitivity to that of the *IRA2-TAP* and wild-type strains. Figure 1B (rows 2 and 4) shows that the *IRA2-TAP* yeast strain has a heat shock phenotype similar to that observed in wild-type cells but that the *ira2-TAP*Δ yeast strain has a heat-sensitive phenotype (row 1). We conclude that the *IRA2-TAP* strain is functional compared to the nonfusion *IRA2* wild-type strain and that the TAP-tagged fusion protein does not impair Ira2 activity.

Next, we performed a tandem affinity purification of Ira2-TAP protein. Cell extracts from the *IRA2-TAP* cells were isolated as described previously (14), and after two rounds of affinity purification, protein complexes bound to the Ira2-TAP protein were separated by gel electrophoresis, digested with trypsin, and analyzed by liquid chromatography-tandem mass spectrometry (Fig. 1C and Table 2). The data revealed both previously known and novel binding partners of Ira2. We found both Ira1 and Ira2 in the mass spectrometry analysis as well as the chaperone MSI3, which had previously been reported to bind to Ira2. Rim15, a component of the Ras-cAMP pathway, was also bound to Ira2 (36, 39). Proteins involved with glycolysis and the production of ATP, including pyruvate kinase, phosphoglycerate kinase, the ATP synthase beta subunit, and ADP/ATP carrier protein 2, were found in the Ira2-bound complex. Interestingly, we found that Ira2 binds to prohibitin, an evolutionarily conserved protein required for Ras-induced c-Raf activation in mammalian cells (31). Furthermore, Asc1, a yeast homolog of human RACK1 which contains WD40 repeats, also binds to Ira2. PKC has been shown to regulate neurofibromin and Ras signaling in mammalian systems (24). Interestingly, Asc1 has recently been shown to function as a Gβ subunit for Gpa2 (44). Of interest is the Gβ mimic Kelch repeat protein 1 (Gpb1), which we found to be abundantly bound to Ira2.

Recently, Gpb1 and Gpb2 were identified as components of the Ras signaling pathway in yeast on the basis of their interaction with Ira1 and Ira2. It was reported that deletions of the *GPB1* and *GPB2* genes resulted in Ira protein instability and a marked increase in RasGTP levels, and therefore, it was proposed that Gpb1/2 positively regulate Ira1 and Ira2 activity (15). Ras activation is usually associated with high cAMP levels in yeast cells (40). However, when using yeast strains deficient in both *GPB1* and *GPB2*, another group could not detect any increase in cAMP levels (29). Since we found association between the Gpb1 and Ira2 proteins in the proteomic analysis, we focused exclusively on the relationship between Gpb1 and Ira2. We generated yeast strains that endogenously expressed both Gpb1-TAP and Ira2-FLAG (*IRA2-3FLAG*/*GPB1-TAP*) and verified protein expression by immunoblotting (Fig. 1D). We confirmed interactions between Ira2 and Gpb1 by performing immunoprecipitation and immunoblotting experiments (Fig. 1E). Association between Ira2 and Gpb1 was further investigated by *in vitro* translation and immunoprecipitation experiments. GFP-tagged Gpb1 and V5-tagged Ira2 were *in vitro* translated and immunoprecipitated with anti-V5 monoclonal antibody. We found that Ira2 efficiently interacts with Gpb1 in the *in vitro* translation and binding experiments (Fig. 1F). Taken together, the results confirm that Ira2 interacts with Gpb1 both *in vitro* and *in vivo*.

Gpb1 negatively regulates Ira2. A previous study showed that Gpb1 and Gpb2 positively regulate Ira1 and Ira2 (15);

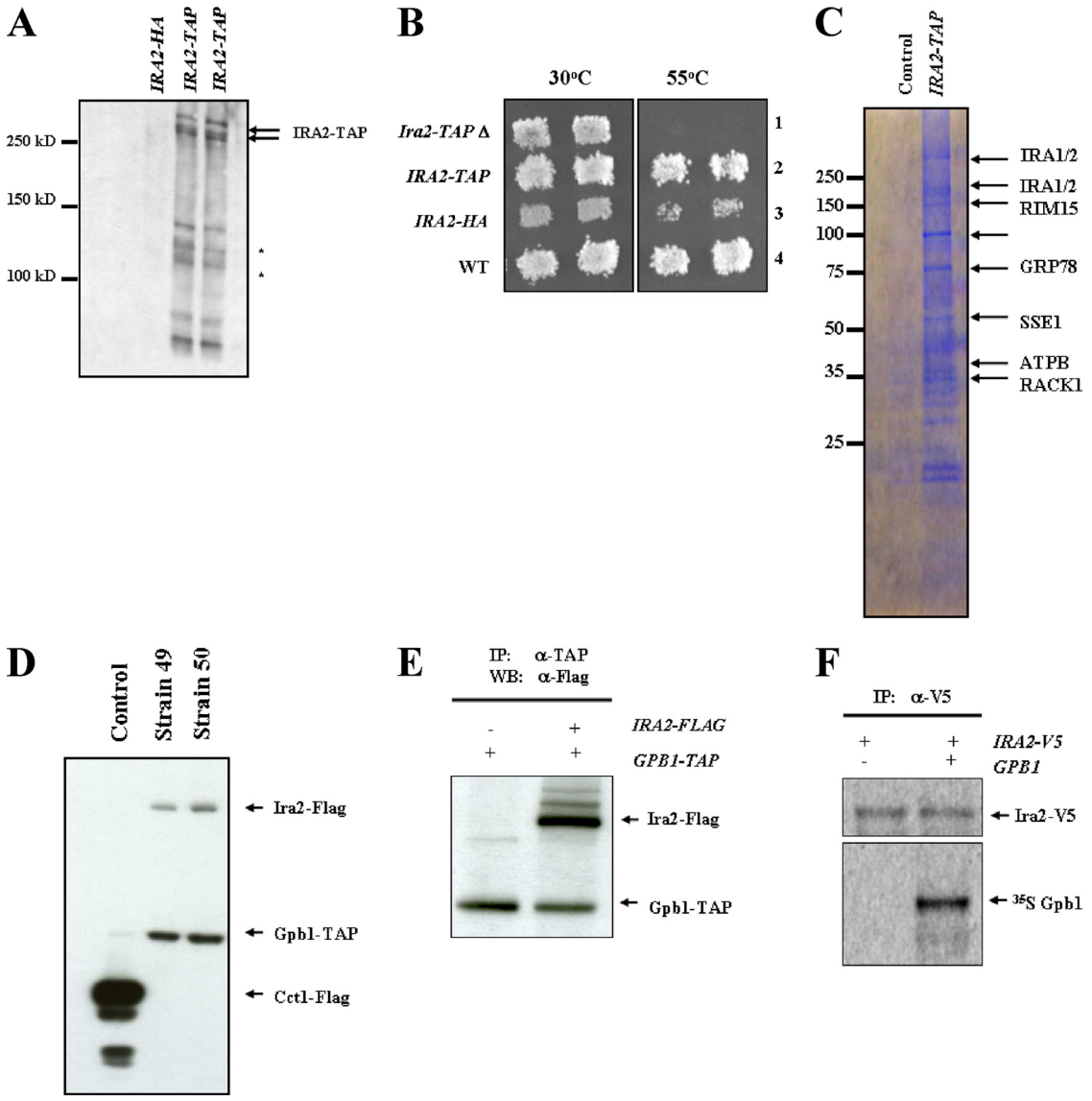

FIG. 1. Characterization of the *IRA2-TAP* yeast strain and identification of the Kelch repeat protein Gpb1 as a negative regulator of Ira2. (A) Soluble extracts from cells expressing the indicated Ira2-HA or Ira2-TAP fusion proteins (replicate samples) were mixed with SDS-PAGE sample buffer and resolved by NuPAGE (Invitrogen) and immunoblotted for the TAP fusion protein. An asterisk represents the different isoforms of the Ira2-TAP protein with the predicted molecular masses. (B) Heat shock experiments were performed on yeast strains as indicated. Cells were grown in a 30°C chamber for 3 days, replica plated, and either unexposed or exposed to a 55°C heat chamber. Photographs were taken 3 days after heat exposure. The Ira2-TAP fusion protein is expressed under its endogenous promoter in a strain with *IRA2* deleted by genetic homologous recombination (row 1), a wild-type strain expressing the Ira2-TAP fusion protein (row 2), a wild-type strain expressing the Ira2-HA fusion protein (row 3), and a wild-type strain that is not tagged (row 4) (strains VP2TPD2, IRA2TAP, IRA2HA, and S288c, respectively). (C) Ira2-TAP fusion protein was copurified from the IRA2TAP yeast strain, and protein complexes were resolved by gel electrophoresis and identified by mass spectrometry (Table 2). The control sample was from a wild-type yeast strain that was not tagged. (D) Yeast strains doubly expressed endogenous Ira2-Flag and Gpb1-TAP fusion proteins. Western blots showed either the control yeast strain expressing Cct1-Flag or two different strains expressing Gpb1-TAP/Ira2-Flag. The *GPB1-TAP* yeast strain was used to create the double-epitope-tagged *GPB1-TAP*/*IRA2-3FLAG* yeast strains 49 and 50 (strains VPG1TP2F, 49, and 50). The *CCT1-3FLAG* yeast strain was used as a control (VPCT13F). Genetic integration experiments were performed using plasmids from a previously described publication (22). (E) Endogenous Gpb1 and Ira2 interaction. Yeast cells (strain VPG1TP2F) expressing Gpb1-TAP and Ira2-Flag fusion proteins were immunoprecipitated (IP), followed by Western blotting (WB) with anti-TAP (α-TAP) and anti-Flag antibodies as indicated. (F) Ira2 and Gpb1 interaction *in vitro*. Ira2-V5 and Gpb1-GFP were translated *in vitro*, subjected to immunoprecipitation (IP) with anti-V5 antibody, and visualized with a Storm 860 PhosphorImager.

however, in our experimental system, we found that deletion of *GPB1-TAP* in the *IRA2-3FLAG*/*GPB1-TAP* yeast strain resulted in a 3-fold increase in Ira2 compared to the level for the wild-type strain (Fig. 2A). Since our results were contrary to previously reported data (15), we repeated our genetic deletions of the *GPB1-TAP* open reading frame (ORF) and obtained two independent yeast strains that have deletions in the *GPB1* allele. Again, we found that *gpb1*Δ mutants possessed

TABLE 2. Report for mass spectrometry data for Ira2 protein binding complexes

S. cerevisiae protein identified[a]	% Sequence coverage
Heat shock protein YG100	48
Phosphoglyerate kinase	36
RIM15	36
Inhibitor regulatory protein IRA2	32
GPB1	28
Pyruvate kinase 1	28
Mannose-1-phosphate guanyltransferase	25
Prion protein RNQ1	23
Prohibitin	21
Enolase	20
RACK1	19
Fructose-bisphosphate aldolase	18
ATP synthase beta chain	17
ADP, ATP carrier protein 2	16
Chaperone protein MSI3	14
GRP78	13
Glycyl-tRNA synthetase	12
V-ATPase A subunit	10
URA1	9
Inhibitor regulatory protein IRA1	8

[a] Proteins were identified from two independent mass spectrometry experiments using the Ira2-TAP fusion protein to pull down the protein complexes.

higher Ira2 protein levels than wild-type cells (Fig. 2A, lanes marked 7 and 10). To test whether the *GPB1-TAP* strain might contain suppressor genes or the Gpb1-TAP fusion protein that could directly modulate Ira2 level and activity in the wild-type strain (*GPB1-TAP*) might not be functional, we performed qRT-PCR to detect the transcriptional activities of two stress genes (*CTT1* and *HSP12*) that had been described to be the direct targets of Ras activation (4, 29). We found that the transcription activities of *CTT1* and *HSP12* in a nontagged WT strain and the *GPB1-TAP* strain are comparable, suggesting that the GPB1-TAP strain behaves like a wild-type strain. Importantly, we found that the *CTT1* and *HSP12* transcriptional levels in the Ira2-deleted strain (*GPB1-TAP* Δ*ira2*) are greatly reduced (Fig. 2B). Therefore, we concluded that the Gpb1-TAP fusion protein is functional and that the *GPB1-TAP* strain does not contain suppressor genes that regulate Ira2 stability. To further investigate the biological activity of Gpb1 in the Ira2/Ras signaling pathway, we cloned *GPB1* under the *GAL1* promoter. We reasoned that if Gpb1 is a negative regulator of Ira2 then overexpression of Gpb1 would downregulate Ira2 and activate Ras. The p*GAL1-GPB1-V5* construct was expressed in the *IRA2-3FLAG*/*gpb1*Δ strain. After 3 h of galactose induction, we found that overexpression of Gpb1-V5 extensively reduced Ira2 protein levels. Furthermore, overexpression of Gpb1-V5 resulted in an increase in RasGTP levels (Fig. 2C).

To further examine Gpb1 activity *in vivo*, we constructed mutant yeast strains in which *IRA1*, *IRA2*, or *IRA1*/*IRA2* is deleted. We overexpressed Gpb1 in these mutant strains and examined their sensitivity to high temperature. We found that expression of GPB1-V5 increased heat sensitivity in the *ira1*Δ/*IRA2* yeast strain compared to the level for a control plasmid (Fig. 2D, ∗). We could not determine the level of heat sensitivity in the *ira2*Δ/*IRA1* mutant strain in the presence of Gpb1, because of the higher degree of heat shock sensitivity in this strain than in the *ira1*Δ/*IRA2* strain in the same experiment (Fig. 2D). One concern is whether the V5 peptide fused to Gpb1 (p*GAL-GPB1-V5*) could interfere with the Gpb1 Kelch domain and acts as dominant negative, thereby causing the phenotypes that we observed. Therefore, we cloned the *GPB1* open reading frame, including the stop codon encoding amino acid (aa) 897 of Gpb1, into the pGAL plasmid, thereby preventing the V5 protein fragment from fusing into Gpb1. When the nontagged p*GAL-GPB1* plasmid is overexpressed in a wild-type yeast strain, we observed a heat shock sensitivity phenotype similar to that observed for a control plasmid (Fig. 2E). This result is consistent with the heat shock phenotype that we obtained when expressing the p*GAL-GPB1-V5* plasmid (Fig. 2D and 3B). Furthermore, overexpression of the nontagged *GPB1* construct greatly repressed *CTT1* and *HSP12* transcription activities, indicative of Ras activation (Fig. 2F). To further demonstrate that the Gpb1-V5 or Gpb1-TAP fusion proteins functioned normally and that the C-terminally tagged fusion proteins did not interfere with Gpb1 functions, we performed genetic complementary experiments in the *IRA2-3FLAG*/*gpb1*Δ yeast strain to determine whether the *GPB1-V5* and *GPB1-TAP* constructs could restore Ira2 protein levels similar to that of the nontagged *GPB1* wild-type construct. Figure 2G shows that expression of either wild-type *GPB1*, *GPB1-V5*, or *GPB1-TAP* under the *GPB1* endogenous promoter fully restored Ira2 protein levels in the mutant *IRA2-3FLAG*/*gpb1*Δ yeast strain. Given these results, we believe that C-terminal tagged V5 or TAP fusion proteins do not interfere with normal Gpb1 functions and that the p*GAL-GPB1-V5* construct is functionally similar to the wild-type construct.

To further address the idea that overexpression of Gpb1 could induce heat shock sensitivity and activate Ras signaling in yeast, we generated a mutant construct that lacks the N-terminal domain, Gpb1 NΔ. We found that overexpression of Gpb1 NΔ failed to induce the heat shock phenotype usually associated with Ras activation (Fig. 3B). Further, overexpression of Gpb1 NΔ caused an increase in *HSP12* transcriptional activity compared to the level for a control plasmid, suggesting that deletion of the Gpb1 N-terminal domain hinders Gpb1 activity (Fig. 3C). Taken together, our results demonstrate that Gpb1 is a negative regulator of Ira2.

Gpb1 and Gpb2 have opposite functions. Previous reports suggested that Gpb1 and Gpb2 positively regulate Ira proteins in yeast (15, 16). However, we observed that Gpb1 negatively regulates endogenous Ira2 protein levels when overexpressed in cells (Fig. 2C) and that Ira2 is upregulated in *gpb1*Δ cells (Fig. 2A). Gpb1 and Gpb2 possess similar Kelch repeat domains at their C termini (35% homology) but contain unique N-terminal domains. To determine whether Gpb2 possesses functions similar to those of Gpb1 in regulating Ira2 activity, we overexpressed p*GAL1-GPB1-V5* and p*GAL1-GPB2-V5* in the *IRA2-3FLAG*/*gpb*Δ yeast strain (VP2.3FDG1) and performed immunoblotting experiments to determine the Ira2 protein levels. We found that Gpb2 overexpression modestly increases Ira2 levels but that overexpression of Gpb1 downregulates Ira2 (Fig. 4A). To further investigate the differences between Gpb1 and Gpb2 *in vivo*, we overexpressed a control, p*GAL1-GPB1-V5*, or p*GAL1-GPB2-V5* plasmid in the wild-type, *ira2*Δ/*IRA1*, *ira1*Δ/*IRA2*, or *ira1*Δ *ira2*Δ strain (W303, VPD1, VPD2, or VPD1.2, respectively) and assessed the heat

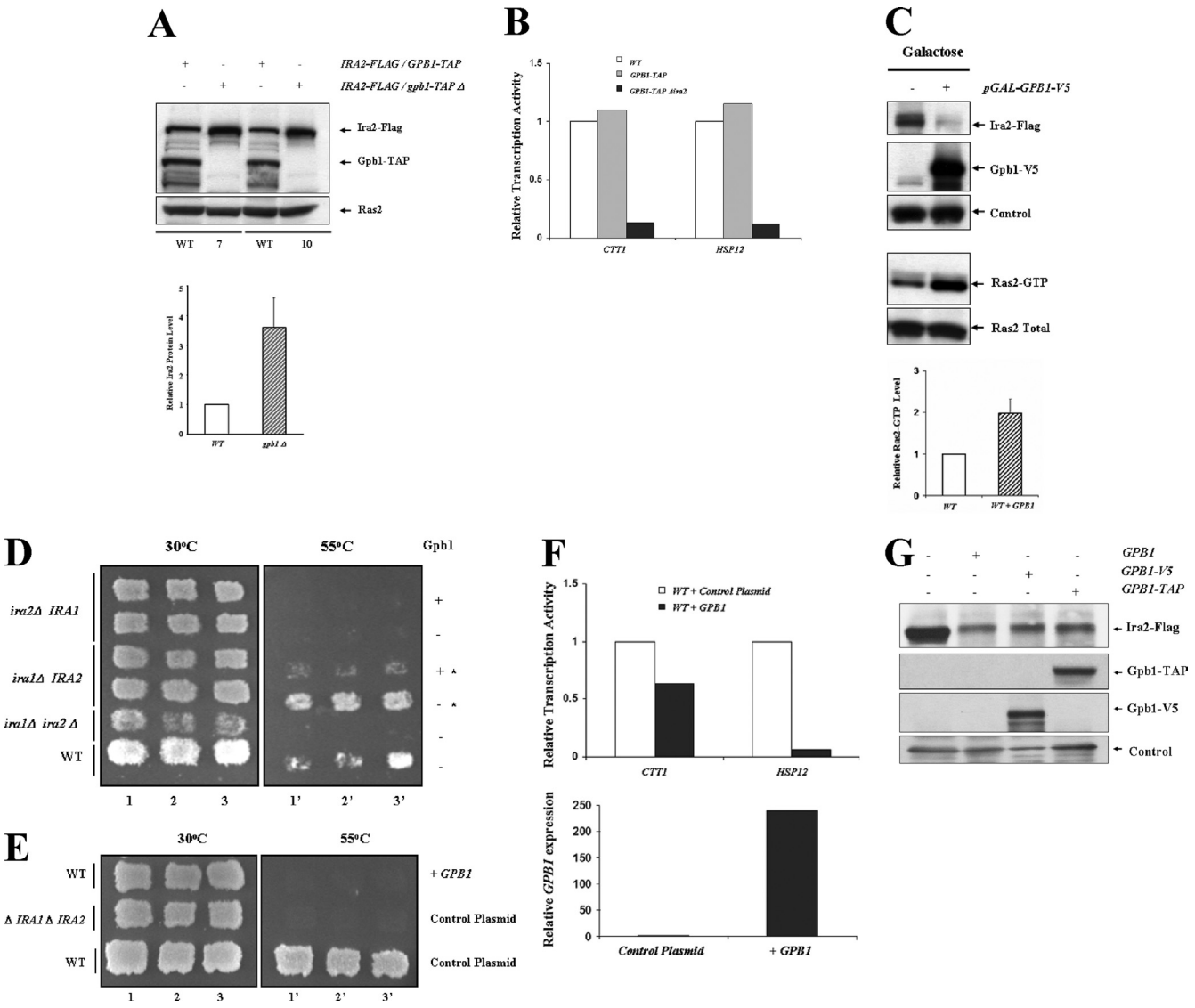

FIG. 2. Gpb1 negatively regulates Ira2 in yeast. (A) Gpb1 deletion increases Ira2 levels. Lysates from either wild-type (WT) or *gpb1*Δ (lanes marked 7 and 10) cells were normalized and subjected to Western blotting with anti-Flag or anti-TAP antibodies (S288c, VP2.3FDG1.7, or VP2.3FDG1.10, respectively). The membrane was blotted with anti-Ras2 antibody to control for equal protein loading. Ira2 protein levels were quantified from three independent experiments with either the wild-type (WT) strain or *gpb1*Δ mutants and are expressed as means ± standard errors of the means. (B) Gpb1-TAP fusion protein is functionally normal and does not activate Ras-targeted genes. The expression levels of *CTT1*, *HSP12*, *GPB1*, and *ACT1* (as an internal standard) were measured by quantitative RT-PCR. The wild-type parental strain S288c (ATCC 201388; *MAT***a** *his2*Δ*1 leu2*Δ*0 met15*Δ *ura3*Δ*0*) or the *GPB1-TAP* or *GPB1-TAP ira2*Δ (VPG1TPD2) strain was grown, and RNA was extracted as described in Materials and Methods. (C) Gpb1 overexpression decreases Ira2 stability and activates Ras signaling. The p*GAL-GPB1-V5* plasmid was transformed into the *IRA2-3FLAG*/*gpb1*Δ yeast cells (VP2.3FDG1.7) endogenously expressing Ira2-Flag. Cells were induced with galactose for 3 h and subjected to immunoblotting with anti-Flag and anti-V5 antibodies to determine protein levels. The lower panel shows Ras2GTP levels in cells overexpressing Gpb1-V5. Pulled-down RasGTP samples from total lysates were subjected to immunoblotting with anti-Ras2 antibody. Total Ras2 levels were subjected to Western blotting for comparison. Ras2GTP levels in wild-type (WT) cells and wild-type cells with Gpb1 overexpression (WT+Gpb1) were quantified from three independent experiments and are expressed as means ± standard errors of the means. (D) Overexpression of Gpb1-V5 in the *ira1*Δ/*IRA2* mutant yeast strain causes heat sensitivity. Galactose induced expression of Gpb1 in either *ira2*Δ/*IRA1*, *ira1*Δ/*IRA2*, *ira1*Δ/*ira2*Δ, or wild-type yeast cells (VPD1, VPD2, VPD1.2, or W303, respectively). To assay for heat shock sensitivity, cells were replica plated onto GAL-Ura3 plates and exposed to a high-temperature chamber (55°C) for 60 min or unexposed to a heat chamber (30°C). Plates were then cooled at room temperature for 30 min and incubated at 30°C for 3 to 7 days before pictures were taken. (E, F) Overexpression of full-length nontagged *GPB1* in the W303 wild-type strain causes heat sensitivity and suppresses Ras-targeted genes. Galactose-induced expression of Gpb1 causes heat sensitivity in WT cells compared to the level for cells that received an empty plasmid. The *ira1*Δ/*ira2*Δ mutant strain (VPD1.2) is included as a control. To assay for heat shock sensitivity, cells were replica plated onto GAL-Ura3 plates and exposed to a high-temperature chamber (55°C) for 60 min or unexposed to a heat chamber (30°C). Plates were then cooled at room temperature for 30 min and incubated at 30°C for 3 to 7 days before pictures were taken. For quantitative qRT-PCR, W303 wild-type (WT) cells that had received nontagged *GPB1* or control plasmids were grown overnight and galactose induced for 3 h to determine the expression of *CTT1*, *HSP12*, *GPB1*, and *ACT1* (as an internal standard). (G) Expression of Gpb1, Gpb1-V5, or Gpb1-TAP under the *GPB1* endogenous promoter in the *IRA2-3FLAG*/*gpb1*Δ yeast strain restored Ira2 protein levels (strain VP2.3FDG1). The *IRA2-3FLAG*/*gpb1*Δ was transformed with a control plasmid or plasmids expressing endogenous *GPB1*, *GPB1-V5*, or *GPB1-TAP*. The three constructs were expressed under the control of the endogenous *GPB1* promoter. Total cell lysates with equal protein concentrations were subjected to immunoblotting (WB) with anti-Flag, anti-TAP, or anti-V5 antibodies. The membrane was blotted using anti-Ydj1 antibodies to control for equal protein loading.

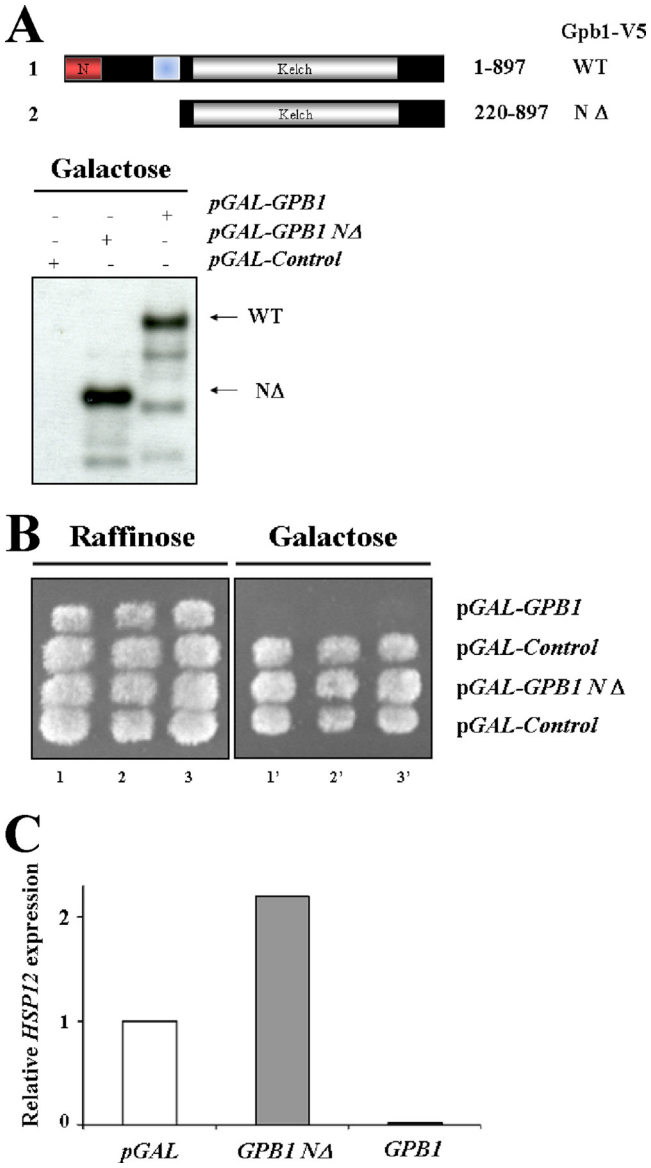

FIG. 3. Expression of Gpb1-V5 fusion protein activates Ras-targeted genes and induces heat sensitivity in yeast. (A) Diagrams show full-length Gpb1 and N-terminally truncated Gpb1. Protein levels of Gpb1-V5 WT and Gpb1 NΔ-V5 were determined by immunoblotting with anti-V5 antibody. (B) Galactose-induced expression of p*GAL-GPB1-V5* results in heat sensitivity in W303 wild-type yeast cells compared to the level for cells that received an empty control or p*GAL-GPB1 NΔ-V5* plasmid. To assay for heat shock sensitivity, cells were replica plated onto GAL-Ura3 plates and exposed to a high-temperature chamber (55°C) for 60 min or unexposed to a heat chamber (30°C). Plates were then cooled at room temperature for 30 min and incubated at 30°C for 3 to 7 days before pictures were taken. (C) Transcription activity of *HSP12* in the W303 wild-type yeast strain expressed p*GAL-GPB1-V5* and p*GAL-Gpb1 N*Δ. The transcription activity of *HSP12* and *ACT1* (as an internal standard) were measured by quantitative RT-PCR. Cells were grown and galactose induced for 3 h before RNA extraction for quantitative RT-PCR analysis.

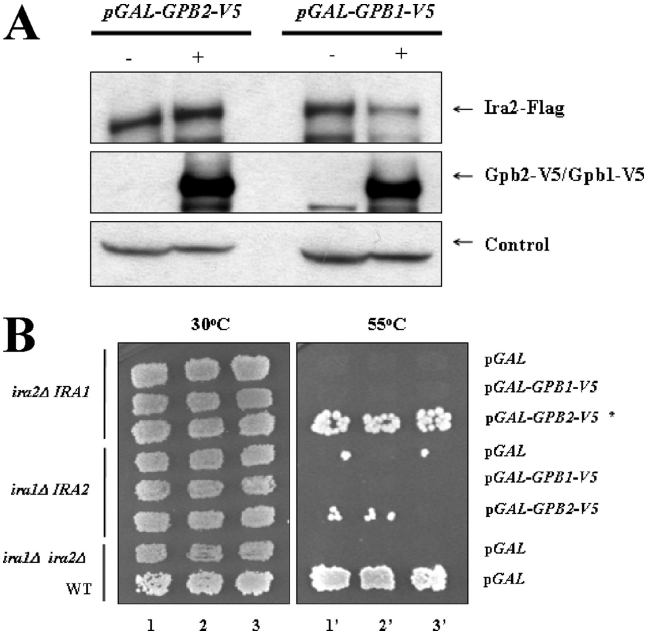

FIG. 4. Gpb1 and Gpb2 have opposite functions. (A) Overexpression of Gpb2 positively regulates Ira2 activity. p*GAL-Gpb2-V5* (2nd lane) or p*GAL-Gpb1-V5* (4th lane) was overexpressed in the *IRA2-FLAG* yeast strain, and cell lysates were subjected to immunoblotting (WB) with anti-Flag or anti-V5 antibodies to detect Ira2, Gpb2, or Gpb1 protein levels. The membrane was blotted using anti-Ydj1 antibodies to control for equal protein loading. (B) Overexpression of Gpb2-V5 in the *ira2*Δ *IRA1* mutant yeast strain causes heat shock resistance. The heat shock sensitivities of the indicated yeast strains, expressing galactose-inducible *GPB1* or *GPB2* and a control plasmid, were compared. Controls cells were either from the *ira1*Δ *ira2*Δ double mutant or from wild-type cells. To assay for heat shock sensitivity, cells were replica plated onto GAL-Ura3 plates and exposed to a high-temperature chamber (55°C) for 60 min or unexposed to a heat chamber (30°C). Plates were then cooled at room temperature for 30 min and incubated at 30°C for 3 to 7 days before pictures were taken.

sensitivity of these. As expected, we found that overexpression of Gpb1 increases heat sensitivity but that overexpression of Gpb2 causes heat resistance in *ira2*Δ/*IRA1* cells (Fig. 4B). This finding suggests that Gpb1 and Gpb2 might have opposite functions and that Gpb1 is a negative regulator of Ira2. Since we identified Gpb1 complexes with Ira2 in our proteomic analysis, we further characterize Gpb1 functions in association with Ira2.

Gpb1 controls Ira2 stability during glucose stimulation. In yeast, glucose stimulation activates the G-protein-coupled receptor Gpr1, which induces adenylyl cyclase activity (11). Glucose-induced activation of Gpr1 stimulates pathways that are critical for cell metabolism and growth (21). Glucose can also induce RasGTP loading in yeast (11, 34). Since Ira2 negatively regulates Ras activity, we hypothesized that in the event of rapid Ras activation induced by stimulation by a nutrient such as glucose, Ira2 protein levels would be tightly regulated. As demonstrated by Cichowski and coworkers, neurofibromin is rapidly degraded upon growth factor stimulation via the ubiquitin-proteasome pathway in mammalian cells (7).

We therefore investigated whether Ira2 is downregulated by glucose stimulation. We treated *IRA2-3FLAG/GPB1-TAP* cells with 5% glucose, and Ira2 levels were assessed by immunoblot analysis. Glucose stimulation triggered Ira2 downregulation within 10 minutes, and a further decrease was observed at 15 min. Interestingly, glucose-induced downregulation of Ira2 was

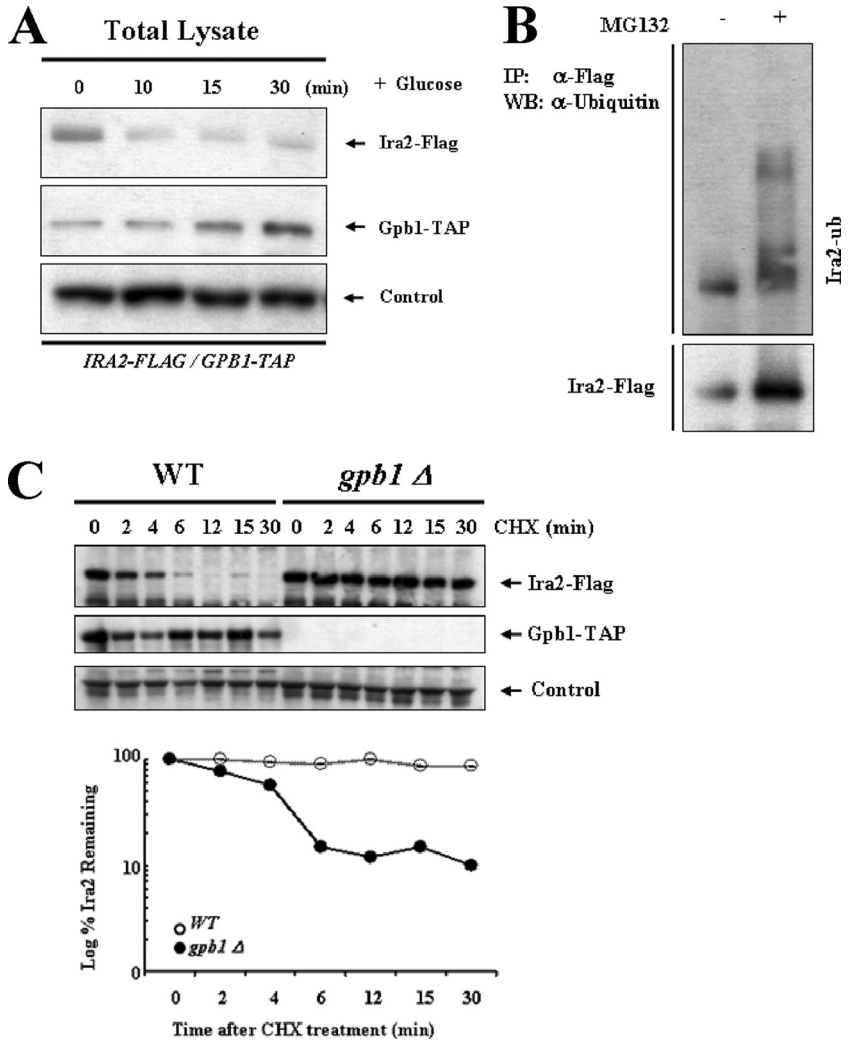

FIG. 5. Gpb1 targets Ira2 for proteasomal degradation in response to glucose. (A) Ira2 is downregulated in response to glucose stimulation. *IRA2-3FLAG/GPB1-TAP* cells (strain VPG1TP2F) were grown to log phase in rich medium overnight and switched to glucose-free medium for 4 to 6 h before 5% glucose stimulation. Ira2 and Gpb1 protein levels were detected by immunoblotting using anti-Flag and anti-TAP antibodies. The membrane was blotted with anti-Ydj1 antibody to control for equal protein loading. (B) Ubiquitination of endogenous Ira2-Flag *in vivo*. *IRA2-3FLAG/GPB1-TAP* cells (strain VPG1TP2F) were either untreated (dimethyl sulfoxide [DMSO]) or treated with the proteasome inhibitor MG132 (10 μM). Cell lysates were immunoprecipitated with an anti-Flag antibody and immunoblotted (WB) with either antiubiquitin or anti-Flag antibodies. (C) Cycloheximide chase assay of Ira2 in wild-type (WT) and *gpb1*Δ (VPG1TP2F and VP2.3FDG1.7, respectively) yeast strains. Ira2 and Gpb1 protein levels were detected by immunoblotting using anti-Flag and anti-TAP antibodies. The membrane was immunoblotted with anti-Ras2 antibody to control for equal protein loading. Protein levels of Ira2 were quantified and are shown for the indicated time points.

accompanied by a gradual elevation of Gpb1 protein levels (Fig. 5A).

Because glucose stimulation or overexpression of Gpb1 downregulated endogenous Ira2, we hypothesized that Gpb1 might be responsible for Ira2 stability and that Ira2 might be ubiquitin modified and degraded to permit rapid Ras activation. To investigate whether Ira2 is a target of the ubiquitination machinery, we treated *IRA2-3FLAG/GPB1-TAP* cells with the proteasome inhibitor MG132, immunoprecipitated Ira2, and immunoblotted with an antiubiquitin antibody. We detected Ira2 ubiquitination after 4 h of MG132 treatment (Fig. 5B).

To test the role of Gpb1 in Ira2 stability, we examined the degradation rate of Ira2 levels in wild-type and *gpb1*Δ mutant cells. Endogenous Ira2 was rapidly downregulated in cycloheximide-treated wild-type cells, while Ira2 was stabilized in *gpb1*Δ mutant cells (Fig. 5C). These results suggest that glucose stimulation induced downregulation of Ira2, possibly by triggering Gpb1-mediated Ira2 ubiquitination and degradation, and confirmed our hypothesis that Gpb1 controls Ira2 stability.

Gpb1 is required for Ira2 ubiquitination and degradation. Gpb1 has a unique N-terminal domain (amino acids 1 to 220) that is not conserved in Gpb2 (16) and a seven β-propeller Kelch repeat domain at its C terminus (amino acids 292 to 816). Previous reports suggest that proteins containing the ubiquitin-like (UBL) and UBA domains can bind to and deliver ubiquitinated proteins to the proteasome for protein degradation. In addition, the Kelch repeat domain has a structure

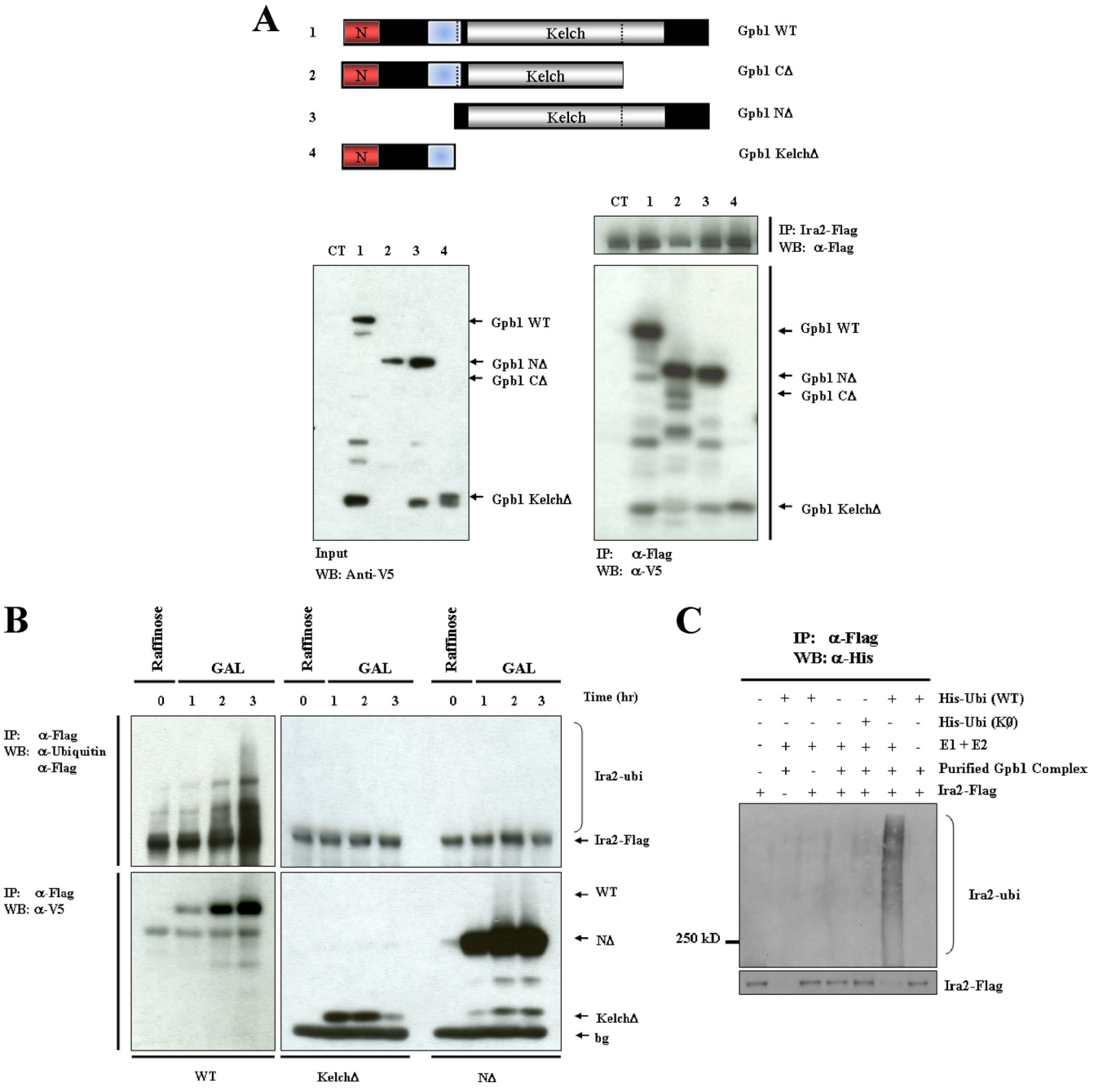

FIG. 6. Full-length Gpb1 targets Ira2 for protein degradation. (A) Diagrams showed the different Gpb1 fragments that were constructed to determine binding to Ira2. Expression levels of full-length Gpb1 and truncated Gpb1 fragments binding to Ira2 are shown. All of the constructed full-length (WT) and truncated Gpb1 fragments were expressed in the *IRA2-3FLAG*/*gpb1*Δ yeast strain (VP2.3FDG1) and galactose induced for 3 h to determine Gpb1 expressions and interactions with Ira2. In particular, the Gpb1 KelchΔ fragment is expressed, as seen in row 4, compared to the level for cells receiving control plasmid (CT). Lysates were collected and immunoblotted with anti-V5 antibody or were subjected to immunoprecipitation (IP) with anti-Flag and immunoblotted (WB) with anti-Flag and anti-V5 antibodies. (B) Gpb1 targets Ira2 for ubiquitination. Overexpression of the Gpb1-V5 wild-type (left), KelchΔ (middle), or NΔ (right) protein was induced in the *IRA2-3FLAG*/*gpb1*Δ yeast strain (VP2.3FDG1.7) by treating cells with galactose at the indicated time points (0 to 3 h). Lysates were collected, subjected to immunoprecipitation (IP) with anti-Flag antibody, and immunoblotted (WB) with antiubiquitin, anti-Flag, and anti-V5 antibodies. (C) *In vitro* ubiquitination of Ira2. The Ira2-Flag and Gpb1-TAP complexes were purified from the *IRA2-3FLAG*/*gpb1*Δ (VP2.3FDG1.7) and *GPB1-TAP*/*ira2*Δ (VPG1TPD2F) yeast strains, respectively, and subjected to an *in vitro* ubiquitination assay. Gpb1 ubiquitination activity was observed in reaction mixtures containing recombinant wild-type His-ubiquitin (His-Ubi) but not in those without the Gpb1 complex, those that received His-ubiquitin with all the lysine amino acids mutated (KØ), or those without E1 and E2. Reaction mixtures were incubated for 1 h, immunoprecipitated (IP) with anti-Flag antibody, and immunoblotted (WB) with anti-His or anti-Flag antibodies.

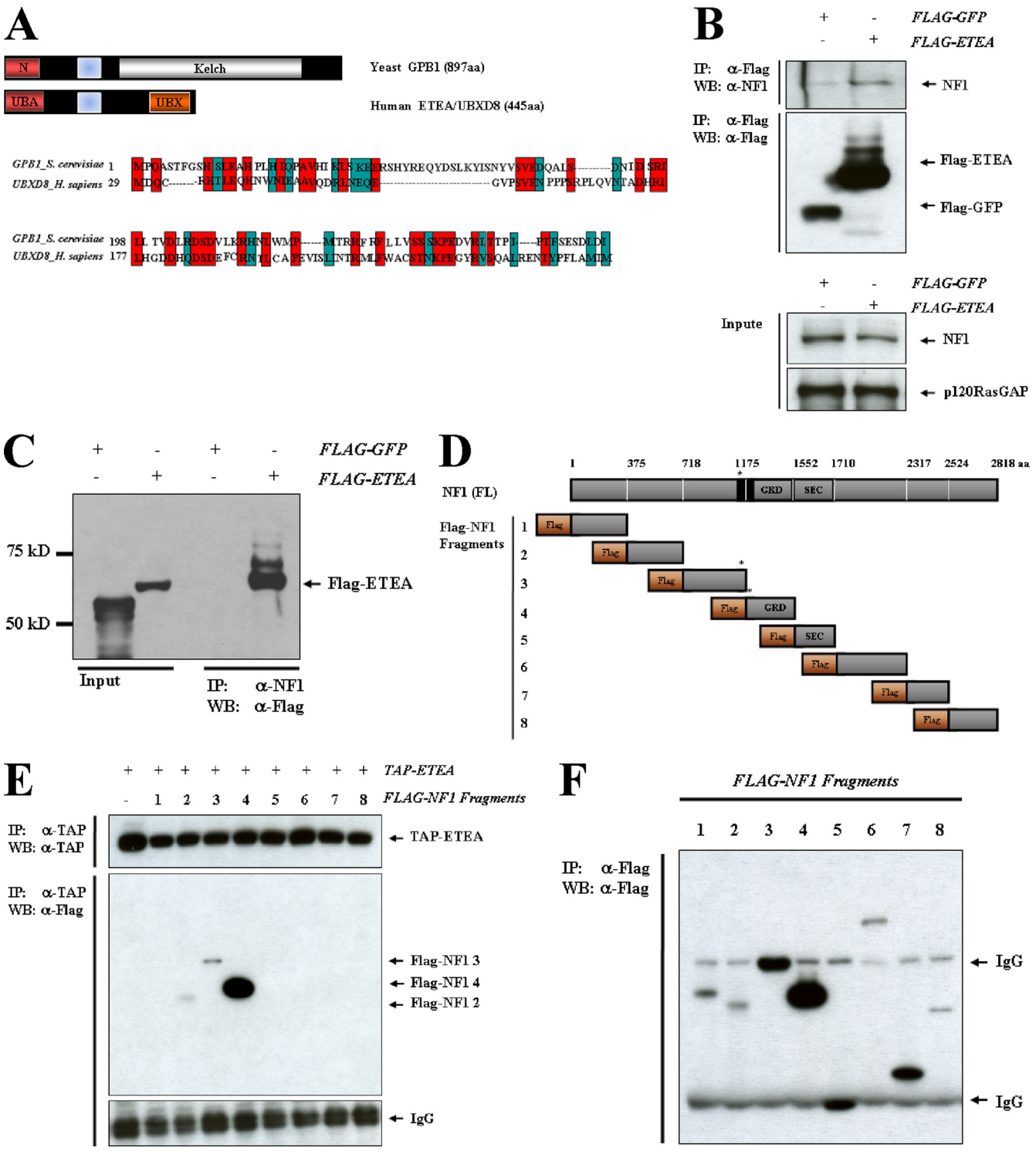

FIG. 7. Identification of ETEA as a UBA-UBX protein that binds to neurofibromin. (A) N-terminal domain alignment of Gpb1 and ETEA. Sequence alignment of the N termini of ETEA and Gpb1, where amino acids shown in red boxes are identical and amino acids shown in blue boxes are similar. The sequence alignment was performed by utilizing the software available at http://www.ebi.ac.uk/ (EMBOSS Align). (B) ETEA binds to endogenous neurofibromin. Flag-GFP or Flag-ETEA was expressed in 293T cells, and equal protein concentrations were subjected to immunoprecipitation (IP) followed by immunoblotting (WB) with anti-Flag and antineurofibromin antibodies. Total lysates were immunoblotted for neurofibromin and p120GAP for control loadings. (C) Direct interactions of neurofibromin with ETEA were determined by immunoprecipitation (IP) with endogenous neurofibromin and immunoblot analysis (WB) with anti-Flag antibody. Neurofibromin interacts with Flag-ETEA but not Flag-GFP. (D, E) Neurofibromin domains bind to ETEA. Flag-tagged NF1 fragments (D) and TAP-tagged ETEA were coexpressed in 293T cells. Total lysates were immunoprecipitated (IP) with anti-TAP antibody and immunoblotted (WB) with anti-Flag or anti-TAP antibodies as indicated to the right. IgG is shown in the lower panel as a loading control. (F) Expression of Flag-tagged neurofibromin fragments. Total lysates were immunoprecipitated (IP) with anti-Flag antibody and immunoblotted (WB) with anti-Flag antibody as indicated on the right.

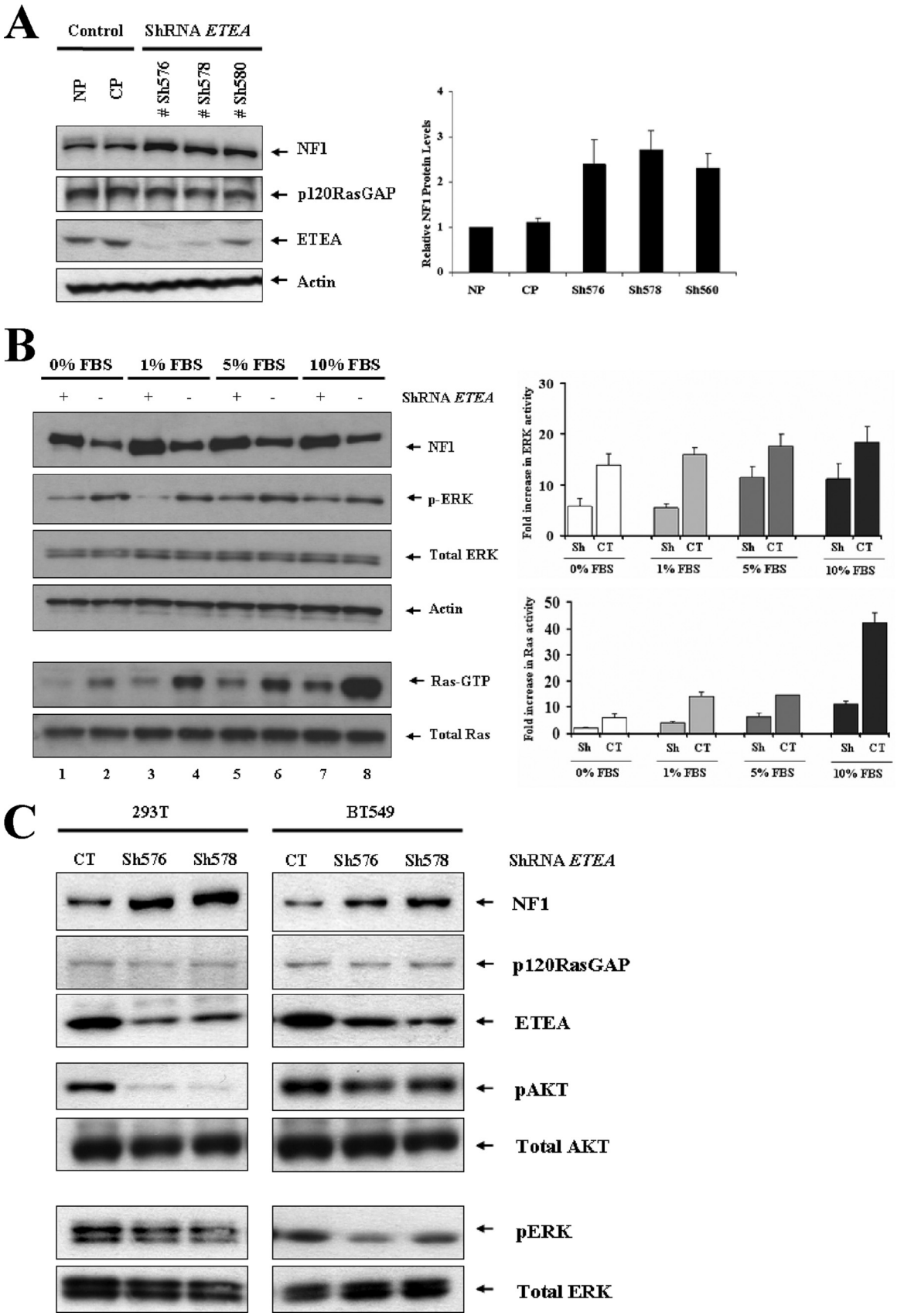

similar to that of the WD40 repeat domain, which is involved in substrate recognition for ubiquitin ligase complexes (17, 41). A recent finding also showed that the Kelch protein KLHL12 binds to the Cullin-3 ubiquitin ligase to negatively regulate the Wnt–β-catenin pathway (1). We generated galactose-inducible plasmids encoding full-length (WT), Kelch-deleted (KelchΔ), C-terminal domain-deleted (CΔ), and N-terminal domain-deleted (NΔ) Gpb1 and expressed these plasmids in the *IRA2-3FLAG/gpb1*Δ yeast strain. We confirmed that the Gpb1 full-length and truncated forms are expressed and interacted with Ira2 by performing immunoblotting and immunoprecipitation experiments (Fig. 6A). To examine the role of Gpb1 in the ubiquitination of Ira2 *in vivo*, we overexpressed Gpb1 WT, Gpb1 KelchΔ, and Gpb1 NΔ in the *IRA2-3FLAG/gpb1*Δ yeast strain at different time points after galactose induction and collected cell lysates for immunoprecipitation and immunoblotting assays. Figure 6B shows that galactose-induced expression of full-length Gpb1 in the *IRA2-3FLAG/gpb1*Δ yeast strain caused an increase in Ira2 ubiquitination in a Gpb1 dose-dependent manner (Fig. 6B, WT). Surprisingly, neither the Gpb1 KelchΔ nor the Gpb1 NΔ fragment promoted Ira2 ubiquitination (Fig. 6B, KelchΔ or NΔ), even though the wild-type, Gpb1 KelchΔ, and Gpb1 NΔ fragments efficiently bind to Ira2. These results suggest that the Kelch and the N domains of Gpb1 are required for Ira2 ubiquitination.

To determine whether Gpb1 can efficiently conjugate ubiquitin to Ira2 *in vitro*, we purified Ira2-Flag and Gpb1-TAP fusion protein complexes from the *IRA2-3FLAG/gpb1*Δ and *ira2*Δ*/GPB1-TAP* mutant strains, respectively, and performed *in vitro* ubiquitin conjugation experiments. We used extensively washed, immunopurified Ira2-Flag as the substrate and purified, TEV-cleaved Gpb1 as the ubiquitin-conjugating enzyme complex. After incubation with either recombinant His-ubiquitin or a recombinant His-ubiquitin mutant (KØ) that has all the lysine residues mutated, Ira2-Flag was immunoprecipitated and immunoblotted with an anti-His antibody to detect Ira2-conjugated His-ubiquitin chains. We found that purified Gpb1 complex can readily promote Ira2 polyubiquitination *in vitro* (Fig. 6C). Given these results, we conclude that the Gpb1 complex ubiquitinates Ira2 *in vivo* and *in vitro*.

ETEA binds and negatively regulates neurofibromin. Neurofibromin can be targeted for proteasome-mediated degradation upon growth factor stimulation (7). We show here that Ira2, the yeast homolog of neurofibromin, is targeted for ubiquitination and proteasomal degradation by Gpb1. Therefore, we hypothesize that there is a functional equivalent to Gpb1 in human cells that is responsible for neurofibromin ubiquitination and degradation. To identify the human homologue of Gpb1, we cloned neurofibromin into eight different fragments (Fig. 7D). With the exception of the GRD and SEC domains, all the fragments were randomly designed and cloned. We chose the GRD (fragment 4) and the SEC (fragment 5) domains to perform the pulldown experiments to identify what proteins interact with these two fragments (6, 12, 42). We then analyzed the pulldown candidates by use of mass spectrometry. Of the neurofibromin binding partners in our analysis, we found ETEA (UBXD8), which contains a UBA domain at its N terminus and a UBX domain at its C terminus.

ETEA was first cloned from CD3-positive blood cells of patients with atopic dermatitis, an inflammatory skin condition characterized by an elevation of eosinophils due to an inappropriate immune response (18). We compared amino acid sequences between ETEA and Gpb1 and found that ETEA and Gpb1 shared some similar amino acid sequences at the N-terminal domains (aa 1 through 31); however, ETEA does not contain a Kelch repeat domain that is present in Gpb1 (Fig. 7A).

To investigate whether ETEA can directly bind to neurofibromin, we expressed Flag-tagged ETEA in 293T cells and performed immunoprecipitation and immunoblotting experiments. We found that ETEA directly binds to endogenous neurofibromin (Fig. 7B and C). To determine which domain of neurofibromin interacts with ETEA, we cotransfected Flag-tagged neurofibromin fragments (fragments 1 through 8) and TAP-ETEA in 293T cells and performed immunoprecipitation assays. Figure 7F shows the protein expression levels of the different neurofibromin Flag-tagged fragments. We found that ETEA directly interacts with three neurofibromin fragments spanning amino acids 372 to 1552. The strongest interaction was with fragment 4 (amino acids 1176 to 1552), which contains the GAP-related domain. Although fragment 4 is highly expressed, it seems that fragments 2, 3, and 4 specifically bind to neurofibromin (Fig. 7E). We also noticed that some of the fragments were not expressed well when transfected into 239T cells (Fig. 7F). This finding is consistent with the previous observations in which neurofibromin fragments containing the neurofibromin GRD were targeted for degradation by the proteasome machinery (7). To investigate whether ETEA can directly bind to the neurofibromin GRD *in vitro*, we utilized a rabbit reticulocyte-based coupled transcription/translation system and performed immunoprecipitation experiments. We found that the neurofibromin GRD directly binds to ETEA

FIG. 8. shRNA targeting *ETEA* expression upregulates neurofibromin protein levels and activity. (A) RNAi targeting *ETEA* transcription increases neurofibromin levels. 293T cells (NP, no plasmid) or 293T stable cell lines expressing a control plasmid (CP) or three different shRNA plasmids (Sh576, Sh578, and Sh580) targeting transcript sequences of *ETEA* were generated. Total lysates were immunoblotted with the antibodies indicated in the right panel. For loading controls, membranes were blotted with anti-p120RasGAP or antiactin antibodies. Quantitative analysis data for neurofibromin levels are expressed as means ± standard errors of the means in the right panel (see Materials and Methods). (B) RNAi targeting *ETEA* transcription inhibits Ras and ERK activities. 293T stable cell lines expressing control (CT) or Sh578 (Sh) plasmids were used to determine Ras and ERK activation at different serum concentrations (0%, 1%, 5%, and 10%). Normalized protein levels were subjected to immunoblotting with the indicated antibodies (left panel). Quantitative analysis data for RasGTP levels and ERK phosphorylation are shown in the right panel (see Materials and Methods). (C) RNAi targeting *ETEA* transcription downregulates AKT phosphorylation in 293T and BT549 cell lines. 293T and BT549 stable cell lines expressing control plasmid (CT) or Sh576 and Sh578 targeting *ETEA* expression were used to determine neurofibromin levels and AKT phosphorylation at a 1% serum concentration. Normalized protein concentrations were subjected to Western blotting with the antibodies indicated (left panel).

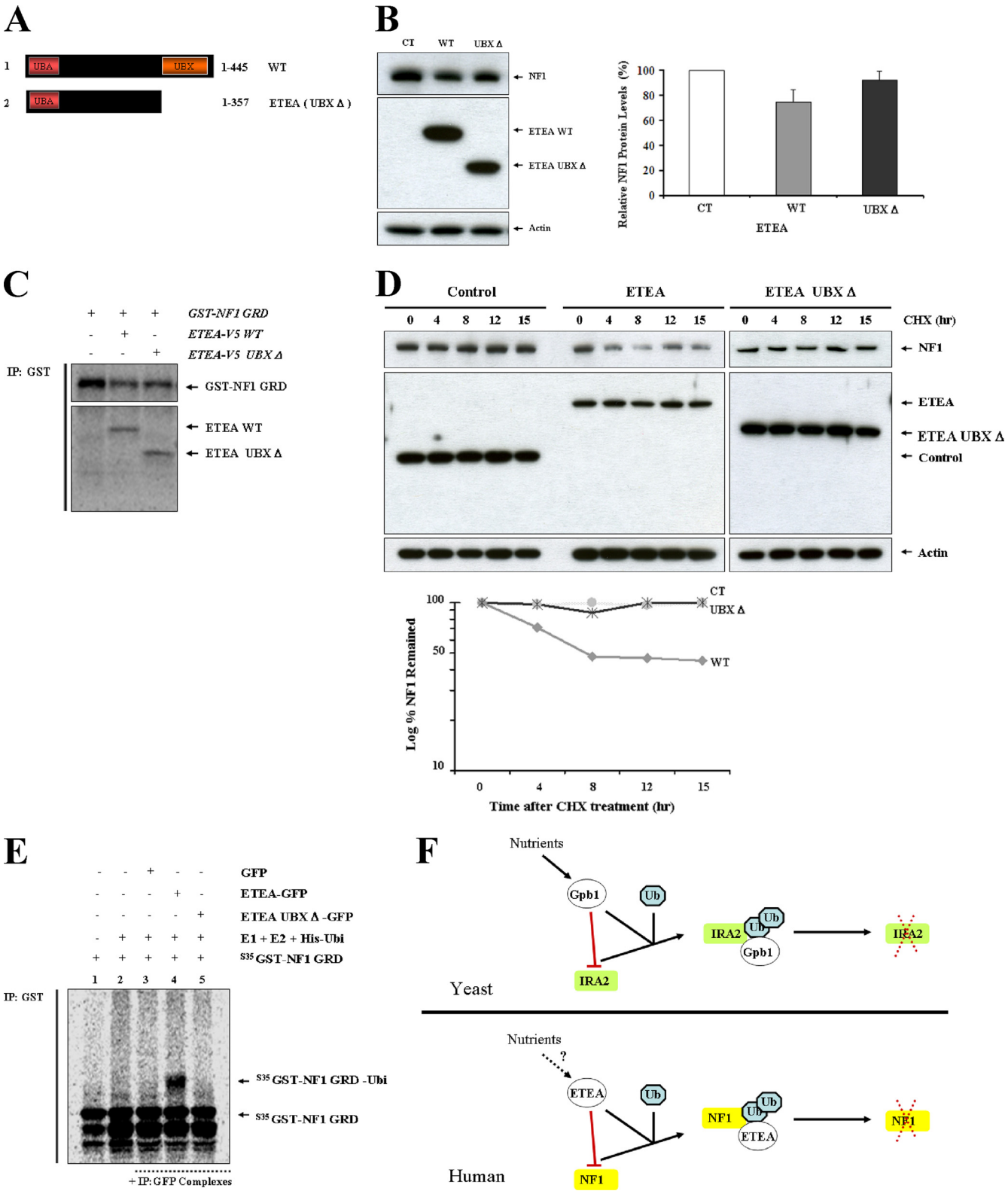

FIG. 9. Functional analysis of ETEA UBX domain. (A, B) Overexpression of full-length ETEA, but not ETEA UBXΔ, reduces neurofibromin levels. 293T cell lysates expressing an empty control (CT), *ETEA-V5* (WT), or *ETEA UBXΔ-V5* (UBXΔ) plasmid were subjected to immunoblotting (WB) with the indicated antibodies. For a loading control, membranes were immunoblotted with antiactin antibody. (C) The neurofibromin GRD binds to both full-length ETEA and ETEA UBXΔ *in vitro*. [^{35}S]methionine-labeled GST-GRD, ETEA-V5, and ETEA UBXΔ-V5 were subjected to coupled transcription/translation with rabbit reticulocyte lysates, coimmunoprecipitated (IP) with Sepharose-conjugated glutathione beads, and visualized with a Storm 860 PhosphorImager. (D) The UBX domain of ETEA controls neurofibromin stability. 293T cells were transfected with

(see Fig. 9C). Therefore, the interaction between ETEA and neurofibromin is direct, and ETEA interacts with neurofibromin within regions that were previously identified as critical for neurofibromin degradation (7).

Silencing of ETEA stabilizes neurofibromin and downregulates Ras activity. We next utilized short hairpin interfering RNAs (shRNAs) to examine whether reducing the expression of ETEA would stabilize neurofibromin. We generated stable cell lines expressing three different shRNA plasmids targeting the human *ETEA* transcription sequences (Sh576, Sh578, and Sh580; Open Biosystems). Compared to the level for control cells, reduced *ETEA* expression by shRNA knockdown resulted in an increase in neurofibromin levels (Fig. 8A). Furthermore, reduced ETEA transcription activity from three independent shRNA constructs causes an increase in neurofibromin protein levels, confirming that the results are consistent and not due to nonspecific targets.

We next investigated whether reduction of *ETEA* expression could downregulate Ras signaling. As shown in Fig. 8B, under nonmitogenic growth conditions (serum concentrations of 0% and 1%), reducing *ETEA* expression markedly downregulated Ras signaling and reduced ERK phosphorylation (Fig. 8B, lanes 1 and 3 versus lanes 2 and 4). At serum concentrations of 5% and 10%, decreased *ETEA* expression in Sh578-expressing cells modestly reduced basal ERK activity compared to the level for control samples (Fig. 8B, lanes 5 and 7 versus lanes 6 and 8). However, RasGTP levels were greatly reduced at 5% and 10% serum concentrations when *ETEA* was repressed in Sh578-expressing cells (Fig. 8B, lanes 5 to 8). Reducing *ETEA* expression in cells plated at a high serum concentration is more effective in reducing Ras activity than in reducing ERK phosphorylation, possibly because Ras is a direct target of neurofibromin whereas ERK is further downstream and can be targeted by multiple receptors that are unrelated to the NF1 pathway. Neurofibromin loss of function leads to Ras activation and deregulation of both the ERK and the AKT pathways (20). We next examined whether targeting ETEA expression could reduce AKT phosphorylation in 293T and BT549 cell lines. Both of these cell lines normally have high basal AKT phosphorylation. We generated 293T and BT549 stable cell lines expressing shRNA that targeted ETEA expression and performed immunoblot analyses to examine AKT phosphorylation levels. As expected, reducing ETEA in both 293T and BT549 cells resulted in upregulation of neurofibromin and a decrease in AKT phosphorylation (Fig. 8C). Taken together, these results demonstrate that neurofibromin stability is controlled by ETEA and that reducing ETEA activity lowers Ras activity and downregulates the ERK and AKT pathways. Furthermore, the data also demonstrate that in cells that have deregulation of AKT, reduced ETEA expression results in downregulation of AKT activity.

The UBX domain of ETEA controls neurofibromin downregulation. Since ETEA directly interacts with neurofibromin at amino acid sites that were previously identified as responsible for neurofibromin stability (7), we hypothesized that ETEA targets neurofibromin for ubiquitination and degradation. To investigate this possibility, we expressed ETEA-V5 (WT) in 293T and examined neurofibromin levels. Overexpression of ETEA caused a decrease in endogenous neurofibromin protein levels (Fig. 9B). ETEA contains both UBA and UBX domains, and while the UBA domain has been shown to bind ubiquitinated substrates and deliver them to the proteasome for protein degradation, the UBX domain has not been fully characterized. Recently, ETEA was found to be an important component of a degradation protein complex and seems to play a role in the recruitment of the AAA ATPase p97. Furthermore, the UBX domain of ETEA might be important for interaction with the AAA ATPase p97 (26). To investigate the mechanism by which ETEA regulates neurofibromin, we generated full-length ETEA and a mutant of ETEA in which the UBX domain is deleted. We overexpressed these constructs in 293T cells and assessed neurofibromin protein levels. Overexpression of the ETEA mutant lacking the UBX domain (ETEA UBXΔ) was less effective in reducing neurofibromin levels than overexpression of full-length ETEA (Fig. 9B). We examined whether the UBX deletion construct could bind to neurofibromin. We expressed the neurofibromin GRD fragment in either wild-type or UBX-deleted ETEA in rabbit reticulocyte lysates and then immunoprecipitated NF1-GRD to assess coimmunoprecipitation of ETEA by immunoblotting. Figure 9C shows that the neurofibromin GRD binds efficiently to both wild-type ETEA and ETEA UBXΔ.

We next investigated the neurofibromin degradation rate by expressing control, ETEA WT, or ETEA UBXΔ plasmids in 293T cells. Cells were treated with cycloheximide to inhibit *de novo* protein translation, and neurofibromin levels were detected by immunoblotting at the indicated times after treatment. We found that the neurofibromin half-life levels were unchanged in control samples under cycloheximide treatments from 1 to 15 h, suggesting that neurofibromin is highly stable. However, overexpression of wild-type ETEA reduced the neurofibromin half-life to 8 h. Surprisingly, neurofibromin levels were fairly stable between 12 and 15 h. In contrast to wild-type ETEA, ETEA UBXΔ did not induce degradation of neurofibromin at the 4-h and 8-h time points (Fig. 9D), supporting our previous observations that ETEA UBXΔ failed to downregulate neurofibromin (Fig. 9B). To examine whether ETEA induced neurofibromin ubiquitination, we purified GFP control,

GST-GFP (CT), *ETEA-V5* (WT), or *ETEA UBXΔ-V5* (UBXΔ). Twenty-four hours after transfection, cells were treated with cycloheximide (CHX) at the time points indicated, and the neurofibromin levels were analyzed by immunoblotting. (E) Wild-type ETEA but not ETEA UBXΔ ubiquitinates neurofibromin *in vitro*. A ubiquitination assay of [^{35}S]methionine-labeled GST-GRD was conducted *in vitro* in the absence or presence of GST-GFP control, ETEA-GFP, or ETEA UBXΔ-GFP protein complexes that were purified from 293T cells. Reactions were performed at 30°C for 90 min. GST-GRD was coimmunoprecipitated (IP) with Sepharose-conjugated glutathione beads, separated by NuPAGE, and visualized with a Storm 860 PhosphorImager. (F) Working model for controlling Ira2 and neurofibromin stabilization by Gpb1 in yeast and ETEA in human cells. (Yeast) Gpb1 negatively regulates Ira2 by inducing Ira2 ubiquitination. During glucose stimulation, Gpb1 ubiquitinates and downregulates Ira2. (Human) ETEA negatively regulates neurofibromin by directly binding and promoting the ubiquitination of neurofibromin.

ETEA-GFP, or ETEA UBXΔ-GFP complexes from 293T cells and performed *in vitro* ubiquitination assays with rabbit reticulocyte lysates expressing ^{35}S-labeled neurofibromin GRD. The wild-type ETEA complex could readily ubiquitinate neurofibromin *in vitro* (Fig. 9E, lane 4), whereas both the GFP and the ETEA UBXΔ-GFP complexes failed to ubiquitinate the neurofibromin GRD (Fig. 9E, lanes 3 and 5). Given these results, we conclude that the ETEA complex ubiquitinates and targets neurofibromin for degradation and that the UBX domain of ETEA is critical for mediating the ubiquitination of neurofibromin.

DISCUSSION

In this study, we utilized an unbiased proteomic approach to identify proteins that interact with and regulate Ira2 and neurofibromin in an effort to identify the novel mechanisms by which these important proteins are regulated. We identified Gpb1 as a protein that binds to Ira2. We found that overexpression of Gpb1 resulted in downregulation of Ira2 but that overexpression of Gpb2 increased Ira2 levels. These observations are in contrast to a reported study which showed that overexpression of both Gpb1 and Gpb2 positively regulates Ira1 and Ira2 and that deletions of Δ*gpb1* and Δ*gpb2* increase RasGTP levels. (15). Other studies have reported inconsistent findings in regard to Gpb1 and Gpb2 functions (27, 29). For example, Ras activation results in downregulation in *HSP12* transcription and causes an increase in cAMP levels. However, at day 1 after cells were grown in yeast extract-peptone-dextrose (YPD), deletion of both *gpb1* and *gpb2* (Δ*gpb1*/Δ*gpb2* yeast strain) did not cause a decrease in *HSP12* transcription or an increase in cAMP production (29). Since Gpb1 and Gpb2 possess similar Kelch repeats at the C-terminal domains but have distinct N-terminal domains, we focused on the N-terminal regions of Gpb1 and Gpb2 to identify differences in the biological functions of the two proteins. Interestingly, we found that the N-terminal domain of Gpb1 has some similarity to ETEA amino acid sequences. Importantly, the N termini of Gpb1 and Gpb2 do not have amino acid sequence similarity to each other compared to the amino acid sequence similarity between Gpb1 and ETEA.

Further, we demonstrated that overexpression of wild-type Gpb1 is critical and sufficient for Ira2 downregulation and Ras activation by promoting ubiquitination of Ira2. Importantly, we found that Ira2 downregulation as well as Ras activation is dependent on the N-terminal domain of Gpb1. In contrast to Gpb1, we found that Gpb2 positively regulates Ira2. Overexpression of Gpb2 modestly increased Ira2 levels, whereas overexpression of Gpb1 had a negative effect on Ira2. Genetic analysis showed that Gpb2 inhibited the heat shock phenotype caused by loss of Ira2 in a heterozygous yeast strain, possibly by causing an increase in Ira1 activity to downregulate active Ras. Importantly, we also found that that overexpression of Gpb1 activates Ras and directly suppressed the expression of several Ras-targeted genes, including *CTT1* and *HSP12*. We addressed the concerns that the Gpb1-TAP or the Gpb1-V5 fusion protein might act as dominant negative by monitoring Ras activity in either the *GPB1-TAP* strain or W303 wild-type cells that received galactose-induced Gpb1. We found that *CTT1* and *HSP12* transcription levels were comparable between the nontagged wild-type and *GPB1-TAP* strains. Furthermore, galactose-induced expression of a nontagged Gpb1 protein induced a heat shock phenotype in the W303 wild-type strain as well as depression of *CTT1* and *HSP12*, indicative of Ras activation. Taken together, these data demonstrate that Gpb1 negatively regulates Ira2 and that Gpb1 and Gpb2 possess different biological functions.

There are several possible explanations for the differences in Gpb1 and Gpb2 functions. One is that Gpb1 and Gpb2 might have two completely different functions but share similar Kelch repeat domains. Many proteins which share similar domain structures but also have different functions have been identified, including the small GTPase family of proteins (8). The yeast *S. cerevisiae* has two RasGAP proteins, Ira1 and Ira2. In addition to regulating Ras, previous reports have pointed out that Ira1 and Ira2 can independently regulate different biological pathways (23, 28). Gpb1 might target Ira2, whereas Gpb2 might target Ira1. Furthermore, proteomic experiments have shown that Gpb1 and Gpb2 bind to different intracellular protein partners, suggesting that these proteins mediate independent signaling pathways (9). Future experiments are needed to address the differences between Gpb1 and Gpb2 functions.

Our working model is supported by previous observations that neurofibromin is negatively regulated by the ubiquitin machinery when cells are stimulated with various growth factors (7). It was postulated that an E3 ligase is responsible for targeting neurofibromin degradation, resulting in rapid activation of Ras. Although the E3 ligase targeting neurofibromin for protein degradation was not identified, amino acid sequences adjacent to the GAP-related domain (GRD) of neurofibromin have been identified and demonstrated to be critical sites for neurofibromin degradation (7). We show here for the first time the identification and functional analysis of a previously unknown UBA-UBX protein that targets neurofibromin for protein degradation. Interestingly, ETEA appears to share some amino acid sequences with the N-terminal domain of Gpb1 but not Gpb2. Loss-of-function analysis revealed that ETEA function is critical for neurofibromin stability. Although more studies are needed to fully address the role of ETEA in neurofibromin regulation, our findings suggest that interfering with ETEA function can increase neurofibromin levels and activity. Remarkably, reducing ETEA activity is effective in lowering active Ras and downregulating the Ras downstream effectors, ERK and AKT. These results suggest that inhibition of ETEA might present a novel opportunity for therapeutic intervention.

ACKNOWLEDGMENTS

We thank Cynthia Mysinger, Amy Young, and Erika Woodbury for critical reading of the manuscript. We thank all of the members of the McCormick laboratory for thoughtful discussion and comments.

The UCSF Mass Spectrometry Facility (A. L. Burlingame, Director) was supported by the Biomedical Research Technology Program of the National Center for Research Resources, NIH NCRR RR015804, NIH NCRR RR001614, and NIH NCRR RR012961. Frank McCormick was supported, in part, by ONYX Pharmaceuticals and UC Discovery grant bio-02-17 10242. Vernon T. Phan is the recipient of the Young Investigator Award from the Children's Tumor Foundation.

REFERENCES

1. **Angers, S., C. J. Thorpe, T. L. Biechele, S. J. Goldenberg, N. Zheng, M. J. MacCoss, and R. T. Moon.** 2006. The KLHL12-Cullin-3 ubiquitin ligase

negatively regulates the Wnt-beta-catenin pathway by targeting Dishevelled for degradation. Nat. Cell Biol. **8:**348–357.
2. **Bader, J. L.** 1986. Neurofibromatosis and cancer. Ann. N. Y. Acad. Sci. **486:**57–65.
3. **Ballester, R., D. Marchuk, M. Boguski, A. Saulino, R. Letcher, M. Wigler, and F. Collins.** 1990. The NF1 locus encodes a protein functionally related to mammalian GAP and yeast IRA proteins. Cell **63:**851–859.
4. **Bissinger, P. H., R. Wieser, B. Hamilton, and H. Ruis.** 1989. Control of Saccharomyces cerevisiae catalase T gene (CTT1) expression by nutrient supply via the RAS-cyclic AMP pathway. Mol. Cell. Biol. **9:**1309–1315.
5. **Boyer, M. J., D. H. Gutmann, F. S. Collins, and D. Bar-Sagi.** 1994. Crosslinking of the surface immunoglobulin receptor in B lymphocytes induces a redistribution of neurofibromin but not p120-GAP. Oncogene **9:**349–357.
6. **Cichowski, K., and T. Jacks.** 2001. NF1 tumor suppressor gene function: narrowing the GAP. Cell **104:**593–604.
7. **Cichowski, K., S. Santiago, M. Jardim, B. W. Johnson, and T. Jacks.** 2003. Dynamic regulation of the Ras pathway via proteolysis of the NF1 tumor suppressor. Genes Dev. **17:**449–454.
8. **Colicelli, J.** 2004. Human RAS superfamily proteins and related GTPases. Sci. STKE **2004:**RE13.
9. **Collins, S. R., K. M. Miller, N. L. Maas, A. Roguev, J. Fillingham, C. S. Chu, M. Schuldiner, M. Gebbia, J. Recht, M. Shales, H. Ding, H. Xu, J. Han, K. Ingvarsdottir, B. Cheng, B. Andrews, C. Boone, S. L. Berger, P. Hieter, Z. Zhang, G. W. Brown, C. J. Ingles, A. Emili, C. D. Allis, D. P. Toczyski, J. S. Weissman, J. F. Greenblatt, and N. J. Krogan.** 2007. Functional dissection of protein complexes involved in yeast chromosome biology using a genetic interaction map. Nature **446:**806–810.
10. **Colombo, S., P. Ma, L. Cauwenberg, J. Winderickx, M. Crauwels, A. Teunissen, D. Nauwelaers, J. H. de Winde, M. F. Gorwa, D. Colavizza, and J. M. Thevelein.** 1998. Involvement of distinct G-proteins, Gpa2 and Ras, in glucose- and intracellular acidification-induced cAMP signalling in the yeast Saccharomyces cerevisiae. EMBO J. **17:**3326–3341.
11. **Colombo, S., D. Ronchetti, J. M. Thevelein, J. Winderickx, and E. Martegani.** 2004. Activation state of the Ras2 protein and glucose-induced signaling in Saccharomyces cerevisiae. J. Biol. Chem. **279:**46715–46722.
12. **D'Angelo, I., S. Welti, F. Bonneau, and K. Scheffzek.** 2006. A novel bipartite phospholipid-binding module in the neurofibromatosis type 1 protein. EMBO Rep. **7:**174–179.
13. **Gettemans, J., K. Meerschaert, J. Vandekerckhove, and V. De Corte.** 2003. A kelch beta propeller featuring as a G beta structural mimic: reinventing the wheel? Sci. STKE **2003:**PE27.
14. **Ghaemmaghami, S., W. K. Huh, K. Bower, R. W. Howson, A. Belle, N. Dephoure, E. K. O'Shea, and J. S. Weissman.** 2003. Global analysis of protein expression in yeast. Nature **425:**737–741.
15. **Harashima, T., S. Anderson, J. R. Yates III, and J. Heitman.** 2006. The kelch proteins Gpb1 and Gpb2 inhibit Ras activity via association with the yeast RasGAP neurofibromin homologs Ira1 and Ira2. Mol. Cell **22:**819–830.
16. **Harashima, T., and J. Heitman.** 2002. The Galpha protein Gpa2 controls yeast differentiation by interacting with kelch repeat proteins that mimic Gbeta subunits. Mol. Cell **10:**163–173.
17. **He, Y. J., C. M. McCall, J. Hu, Y. Zeng, and Y. Xiong.** 2006. DDB1 functions as a linker to recruit receptor WD40 proteins to CUL4-ROC1 ubiquitin ligases. Genes Dev. **20:**2949–2954.
18. **Imai, Y., A. Nakada, R. Hashida, Y. Sugita, T. Tanaka, G. Tsujimoto, K. Matsumoto, A. Akasawa, H. Saito, and T. Oshida.** 2002. Cloning and characterization of the highly expressed ETEA gene from blood cells of atopic dermatitis patients. Biochem. Biophys. Res. Commun. **297:**1282–1290.
19. **Jin, J., E. E. Arias, J. Chen, J. W. Harper, and J. C. Walter.** 2006. A family of diverse Cul4-Ddb1-interacting proteins includes Cdt2, which is required for S phase destruction of the replication factor Cdt1. Mol. Cell **23:**709–721.
20. **Johannessen, C. M., E. E. Reczek, M. F. James, H. Brems, E. Legius, and K. Cichowski.** 2005. The NF1 tumor suppressor critically regulates TSC2 and mTOR. Proc. Natl. Acad. Sci. U. S. A. **102:**8573–8578.
21. **Kraakman, L., K. Lemaire, P. Ma, A. W. Teunissen, M. C. Donaton, P. Van Dijck, J. Winderickx, J. H. de Winde, and J. M. Thevelein.** 1999. A Saccharomyces cerevisiae G-protein coupled receptor, Gpr1, is specifically required for glucose activation of the cAMP pathway during the transition to growth on glucose. Mol. Microbiol. **32:**1002–1012.
22. **Longtine, M. S., A. McKenzie III, D. J. Demarini, N. G. Shah, A. Wach, A. Brachat, P. Philippsen, and J. R. Pringle.** 1998. Additional modules for versatile and economical PCR-based gene deletion and modification in Saccharomyces cerevisiae. Yeast **14:**953–961.
23. **Magherini, F., S. Busti, T. Gamberi, E. Sacco, G. Raugei, G. Manao, G. Ramponi, A. Modesti, and M. Vanoni.** 2006. In Saccharomyces cerevisiae an unbalanced level of tyrosine phosphorylation down-regulates the Ras/PKA pathway. Int. J. Biochem. Cell Biol. **38:**444–460.
24. **Mangoura, D., Y. Sun, C. Li, D. Singh, D. H. Gutmann, A. Flores, M. Ahmed, and G. Vallianatos.** 2006. Phosphorylation of neurofibromin by PKC is a possible molecular switch in EGF receptor signaling in neural cells. Oncogene **25:**735–745.
25. **Martin, G. A., D. Viskochil, G. Bollag, P. C. McCabe, W. J. Crosier, H. Haubruck, L. Conroy, R. Clark, P. O'Connell, R. M. Cawthon, et al.** 1990. The GAP-related domain of the neurofibromatosis type 1 gene product interacts with ras p21. Cell **63:**843–849.
26. **Mueller, B., E. J. Klemm, E. Spooner, J. H. Claessen, and H. L. Ploegh.** 2008. SEL1L nucleates a protein complex required for dislocation of misfolded glycoproteins. Proc. Natl. Acad. Sci. U. S. A. **105:**12325–12330.
27. **Niranjan, T., X. Guo, J. Victor, A. Lu, and J. P. Hirsch.** 2007. Kelch repeat protein interacts with the yeast Galpha subunit Gpa2p at a site that couples receptor binding to guanine nucleotide exchange. J. Biol. Chem. **282:**24231–24238.
28. **Park, J. I., C. M. Grant, and I. W. Dawes.** 2005. The high-affinity cAMP phosphodiesterase of Saccharomyces cerevisiae is the major determinant of cAMP levels in stationary phase: involvement of different branches of the Ras-cyclic AMP pathway in stress responses. Biochem. Biophys. Res. Commun. **327:**311–319.
29. **Peeters, T., W. Louwet, R. Gelade, D. Nauwelaers, J. M. Thevelein, and M. Versele.** 2006. Kelch-repeat proteins interacting with the Galpha protein Gpa2 bypass adenylate cyclase for direct regulation of protein kinase A in yeast. Proc. Natl. Acad. Sci. U. S. A. **103:**13034–13039.
30. **Petroski, M. D., and R. J. Deshaies.** 2005. Function and regulation of cullin-RING ubiquitin ligases. Nat. Rev. Mol. Cell Biol. **6:**9–20.
31. **Rajalingam, K., C. Wunder, V. Brinkmann, Y. Churin, M. Hekman, C. Sievers, U. R. Rapp, and T. Rudel.** 2005. Prohibitin is required for Ras-induced Raf-MEK-ERK activation and epithelial cell migration. Nat. Cell Biol. **7:**837–843.
32. **Riccardi, V. M.** 1992. Type 1 neurofibromatosis and the pediatric patient. Curr. Probl. Pediatr. **22:**66–107.
33. **Rodriguez-Viciana, P., J. Oses-Prieto, A. Burlingame, M. Fried, and F. McCormick.** 2006. A phosphatase holoenzyme comprised of Shoc2/Sur8 and the catalytic subunit of PP1 functions as an M-Ras effector to modulate Raf activity. Mol. Cell **22:**217–230.
34. **Rudoni, S., S. Colombo, P. Coccetti, and E. Martegani.** 2001. Role of guanine nucleotides in the regulation of the Ras/cAMP pathway in Saccharomyces cerevisiae. Biochim. Biophys. Acta **1538:**181–189.
35. **Schubbert, S., K. Shannon, and G. Bollag.** 2007. Hyperactive Ras in developmental disorders and cancer. Nat. Rev. Cancer **7:**295–308.
36. **Shirayama, M., K. Kawakami, Y. Matsui, K. Tanaka, and A. Toh-e.** 1993. MSI3, a multicopy suppressor of mutants hyperactivated in the RAS-cAMP pathway, encodes a novel HSP70 protein of Saccharomyces cerevisiae. Mol. Gen. Genet. **240:**323–332.
37. **Tanaka, K., M. Nakafuku, T. Satoh, M. S. Marshall, J. B. Gibbs, K. Matsumoto, Y. Kaziro, and A. Toh-e.** 1990. S. cerevisiae genes IRA1 and IRA2 encode proteins that may be functionally equivalent to mammalian ras GTPase activating protein. Cell **60:**803–807.
38. **Tanaka, K., M. Nakafuku, F. Tamanoi, Y. Kaziro, K. Matsumoto, and A. Toh-e.** 1990. IRA2, a second gene of Saccharomyces cerevisiae that encodes a protein with a domain homologous to mammalian ras GTPase-activating protein. Mol. Cell. Biol. **10:**4303–4313.
39. **Thevelein, J. M., and J. H. de Winde.** 1999. Novel sensing mechanisms and targets for the cAMP-protein kinase A pathway in the yeast Saccharomyces cerevisiae. Mol. Microbiol. **33:**904–918.
40. **Toda, T., I. Uno, T. Ishikawa, S. Powers, T. Kataoka, D. Broek, S. Cameron, J. Broach, K. Matsumoto, and M. Wigler.** 1985. In yeast, RAS proteins are controlling elements of adenylate cyclase. Cell **40:**27–36.
41. **Welcker, M., and B. E. Clurman.** 2008. FBW7 ubiquitin ligase: a tumour suppressor at the crossroads of cell division, growth and differentiation. Nat. Rev. Cancer **8:**83–93.
42. **Welti, S., S. Fraterman, I. D'Angelo, M. Wilm, and K. Scheffzek.** 2007. The sec14 homology module of neurofibromin binds cellular glycerophospholipids: mass spectrometry and structure of a lipid complex. J. Mol. Biol. **366:**551–562.
43. **Xu, G. F., B. Lin, K. Tanaka, D. Dunn, D. Wood, R. Gesteland, R. White, R. Weiss, and F. Tamanoi.** 1990. The catalytic domain of the neurofibromatosis type 1 gene product stimulates ras GTPase and complements ira mutants of S. cerevisiae. Cell **63:**835–841.
44. **Zeller, C. E., S. C. Parnell, and H. G. Dohlman.** 2007. The RACK1 ortholog Asc1 functions as a G-protein beta subunit coupled to glucose responsiveness in yeast. J. Biol. Chem. **282:**25168–25176.
45. **Zhu, Y., and L. F. Parada.** 2001. Neurofibromin, a tumor suppressor in the nervous system. Exp. Cell Res. **264:**19–28.